We would like to thank Anders Carlson for the comments provided to encourage discussion of how our manuscript could be improved. Please find below our responses to these comments and the changes in the manuscript.

1-Comment from the referee
Sánchez-Montes et al. present new and exciting SST and IRD data from IODP Site U1417 in the Gulf of Alaska spanning 4 to 1.7 Ma. This occurs during the Pliocene to Pleistocene transition when the world shifted into the modern ice age period. By measuring IRD and SST records in the same core, the authors can provide a one-to- one comparison between local temperature and the behavior of tidewater glaciers. While this data is exciting, the paper needs some substantial revisions and consideration of other data not referenced. I'll leave my comments at a more general level at present to guide revision prior to more specific comments.
First, don't call it the mid-Pliocene warm period. The MPWP is actually the mid-Piacenzian warm period. The Piacenzian used to be in the mid Pliocene but as of 2009, it is now the late Pliocene. See Gibbards et al.'s revision of the Cenozoic timescale.

2-Author's response
Thank you for spotting this, we agree this should be changed.

3-Author's changes in the revised manuscript
The MPWP is amended in a revised manuscript to be the acronym of the Mid-Piacenzian Warm Period (see page 1, line 24).

1-Comment from the referee
Second, the authors should skip this comparison with modern SST in their discussion and rather focus on comparing with the alkenone record of Praetorius et al. (2015 Nature) that is from 17 ka-0 ka at what is now Site U1419 (core is EW0408-85JC taken on the site survey cruise for the IODP leg). The core top temp is the same as at U1417, supporting the comparison. And more importantly, the glacial interglacial absolute and relative change at U1419 from 17 to 0 ka is the same as the Pliocene and early Pleistocene range and absolute temps at U1417. I think this rules out a major change in CO2 average composition as a driver of a Pliocene to Pleistocene to last deglaciation SST pattern.

2-Author's response
We could acknowledge the similarity in the range of glacial-interglacial SST changes between the two sites in the manuscript, but with the strong caveat that we would not be comparing like with like. We would like to highlight that U1417 and U1419 are 400 km apart and have around 4 km difference in water depth. As we show on Figure 1 in our original manuscript, presently these sites are under the influence of different oceanic currents: U1417 is influenced by the Alaskan Current and U1419 is influenced by the Alaskan Coastal Current. If we choose to compare U1417 during the 4 to 1.7 Ma time period with U1419 covering the 17 Ka to 0 Ka interval, we would be comparing the behaviour change over time of two different currents (and we do not have LGM- Holocene data from U1417 to make a direct comparison to

U1419). We do not see the benefit of this comparison as an alternative to our current comparison between the modern SSTs at our core site with those of the Pliocene and early Pleistocene. In our manuscript, we prefer to compare Site U1417 with modern SST at the same location (Site U1417), to give information about the degree of change of that particular current under different past climates.

3-Author's changes in the revised manuscript
Reflecting on the reviewer's comments, a sentence in the revised manuscript has been amended to highlight the modern location of Site U1417:

"The location of Site U1417 rests under the modern influence of the AC (Fig. 1)." (Page 3, line 17).

Two additional sentences clarify the benefit of the Pliocene and Pleistocene-present comparison in the revised manuscript:

"We compare our palaeo-SST with the modern SST (here "modern" refers to the averaged decadal statistical mean SST of 6.5 °C (standard deviation of 3.4 °C) during the 1955 to 2012 time period, NOAA WOD13; Boyer *et al*., 2013) at the location of Site U1417 to observe changes in the behaviour of the Alaskan Current." (Page 7, lines 17-20)

"To understand the evolution of the ocean currents governing the North Pacific at the present core sites (Fig. 1) and to find possible explanations of the observed SST distributions during the Pliocene and Pleistocene climate evolution, the modern climate system is used here as an analogue." (Page 13, lines 24-26).

1-Comment from the referee
Third, quit saying this is the Cordilleran ice sheet. IRD only means you have a marine terminating ice margin. There is no Cordilleran ice sheet today and the Gulf of Alaska has a lot of marine terminating ice margins and icebergs floating around. For instance, both Bering and Malaspina glaciers could quickly become marine terminating if a big storm came through and blew away their morainal banks that happen to right now be above sea level. Both glaciers have beds below sea level except for that little bank. The evidence for an ice sheet comes from the dated proglacial gravels to the northeast in Hidy et al. (QSR 2013) that date the first Cordilleran ice sheet to about 2.6 Ma. This paper should be discussed. Likewise, the authors should use the proximal mag sus. record from ODP Site 887 rather than the far removed to western Pacific records of 882 that Haug et al. produced. I would also include comparison of the U1419 mag sun record to 887 to support the authors suggestions/conclusions. The mag sus record could also help in improving the IRD resolution/interpretation. Surprised it isn't included. In summary, the authors should just refer to tidewater glaciation of the mountains, leaving out the word ice sheet or Cordilleran ice sheet. As far as the record they have in U1419, the conclusion is that some icebergs survived to U1419 once at 2.7 Ma and then again after 2.6 Ma. This is important findings but by no means says anything about an ice sheet or its size. The authors could compare IRD abundance to the IRD record from Addison et al.

(2012 Paleoc) on 85JC. Now, 85JC is much closer to the ice margin and coast but could provide some kind of context.

2-Author's response
As we noted in the previous comment, Site U1417 is located at present ~450 km away from the coast. At present, tidewater glaciers have retreated far inland from their advance during the Little Ice Age (Molnia, 2007; 2008). Although icebergs calve into fjords and bays today, they do not survive to reach the Gulf of Alaska. We have found literature on the heavy influence of glacier runoff on the characteristics of the ACC that flows along the NW Alaskan coast (Weingartner et al., 2005; Royer and Grosch, 2006), which today acts as a barrier to icebergs reaching central GOA. Thus, the enhanced iceberg delivery into the GOA during the early Pleistocene requires a more extensive and/or productive calving margin in ice from the Cordillera, than is observed today.

In our multi-proxy data set from Site U1417 we observe notable changes, in addition to peaks in IRD between 3 to 2.5 Ma that support the establishment of the Cordilleran Ice Sheet (CIS). These include a step-wise increase in sedimentation rates, increase meltwater discharge and increase in the delivery of terrestrial leaf-wax lipids. We assert that the observations recorded at U1417 from 3-2.5 Ma indicate widespread glaciation along the Alaskan margin resulting from an expanding CIS with marine-ending outlet glaciers, and not an advance of a singular mountain glacier to tidewater. A previous study (St John and Krissek, 1999) also identified IRD increasing in Site 887, which is located 200 km southwest of U1417. In Figure 2, IRD from both Site 887 and U1417 are plotted. Site U1417 records a higher abundance of IRD than Site 887, which we infer could be due to its proximity to the ice in coastal Alaska (Fig. 1). Mindful of the differences in the age models of the two sites, the IRD peaks show similar increases and decreases during the 4 to 1.7 Ma interval, suggesting a wider distribution of enhanced iceberg delivery to the GOA than might be expected from a single outlet glacier.

Our study advances the understanding of ice rafting in the North Pacific (as discussed in St. John and Krissek, 1999) by considering SSTs as a significant factor in the survivability of icebergs transiting the Pacific Ocean (page 11, lines 24-28 in the revised manuscript). For example, a reduction in SSTs occurs in association with an IRD peak at 2.9 Ma, and several high frequency peaks in IRD from 2.7 to 2.4 Ma are associated with higher and more variable SSTs. The reviewer notes the work of Hidy et al. (2013) and their chronology for the Klondike gravel, which marks the 'earliest and most extensive Cordilleran ice sheet' on its eastern margins. Hidy et al. (2013) use independent cosmogenic nuclide dating to identify the maximum advance of the CIS at 2.64 Ma (+0.20/-0.18 Ma). A large ice advance on land in the eastern Cordillera, at the same time as enhanced IRD delivery to two sites in the North Pacific (U1417, ODP 887) suggest that widespread glaciation had developed in the interval 2.7-2.4 Ma.

Icebergs were calved from the CIS marine-terminating outlet glaciers, which cut troughs across the continental shelf (e.g. shown for the Last Glacial Maximum (LGM) in Fig 1 of Gulick et al., 2015). As noted during the original IODP expedition, the dominance of low-grade metamorphic lithologies suggest that the Chugach metamorphic complex (Jaeger et al., 2014) was a primary source of IRD for Lithological Unit I (Jaeger et al., 2014). Due to the spatial extent of this formation and without further detailed investigation of clast lithologies (and their geochemistry) it is not possible for us to test whether the IRD being deposited at Site U1417 is from one tidewater glacier system or not, although it is not clear why one glacier would advance and generate sufficient IRD in isolation, especially in the context of the

eastward advance onshore detailed by Hidy et al. (2013) discussed above. It is beyond the scope of this study to test this question. However, the TAR, CPI and IRD Rc data we also generated for Site U1417 sediments suggest a mix of sediment sources being eroded, transported and deposited to Site U1417. This further supports an influence of widespread glaciation influencing Site U1417 during the Cordilleran Ice Sheet expansion. Connecting this comment with a comment from Reviewer 2, we propose that including the CPI (carbon preference index) might help in visualising the diversity of material (indicated by the maturity of the sediments) reaching Site U1417 and thus, the diverse provenance of material eroded and transported to Site U1417. The distance of U1417 from the present coastline and the diversity of material arriving to Site U1417 from the terrain strongly suggests a mixed source of organic matter to the Site.
We have cited Gulick et al., 2015 in order to link Site U1417 to the other sites (including U1419) drilled along a transect by IODP Expedition 341. This transect extends from the deep sea to the Alaskan Margin. It is important to note that the high sedimentation rates in this temperate glacimarine setting preclude the direct comparison of the oNHG described in our paper with any other sites drilled closer to the continent (including U1419 and 85JC mentioned by the referee, which do not extend beyond the most recent glacial stage). The response of CIS deglaciation after the LGM has been documented at 85JC on the continental rise by sudden reductions in sedimentation rate, IRD delivery, and bulk density (Davies et al., 2011) but the record does not extend to the onset of glaciation during the last marine isotope stage. In response to the reviewer's concerns, we can include additional comparison of our data for the Pliocene/early Pleistocene at Site U1417 with the late Pleistocene data of Sites U1419 / 85JC, but with the caveat that these are quite different sedimentary environments and timescales (as evident by the different range of sedimentary N/C vs δ13C (‰) signature at 85JC and U1417).

3-Author's changes in the revised manuscript
We have replaced the Haug et al., 2005 citation with the Hidy et al., 2013 reference:

"The later onset (oNHG) or intensification (iNHG) of the Northern Hemisphere Glaciation is marked by the expansion of the Laurentide, Greenland and Scandinavian ice sheets around 2.5 Ma indicated by ice rafted debris (IRD) records from the North Atlantic Ocean (i.e. Shackleton *et al*., 1984) and the advance of the Cordilleran Ice Sheet at 2.7 Ma inferred from a terrestrial record (Hidy *et al*., 2013)." (Page 2, line 4)

We have included Hidy et al. (2013)'s reference in our revised manuscript to support the attribution of our IRD advance to the Cordilleran Ice Sheet expansion:

"The timing of the increase in IRD at Site U1417 coincides with the increase in IRD at Site 887 (St John and Krissek, 1999) and the maximum extent of the CIS as recorded onshore in the eastern Cordillera by the extensive Klondike gravels at 2.64 Ma (+0.20/-0.18 Ma) (Hidy et al., 2013)." (page 11, line 25).

We have included Hidy et al, 2013's Lower Klondike Valley and ODP 887 locations in Figure 1b and c.

The age of the CIS glaciation in Yukon interior (Hidy et al., 2013) (purple vertical line) and the IRD MAR record at ODP 887 (Fig. 2d) are now included in Fig. 2.

We have clarified the overall increasing terrestrial organic matter trend through the Pliocene and Pleistocene

“Terrigenous and aquatic organic matter sources increase during the early Pleistocene in comparison with the late Pliocene.” (page 5, line 9).

and linked it to the CIS glaciation

“The most reasonable explanation is that the land was becoming increasingly ice covered, so that the erosion of vegetation and terrigenous organic matter eroded and transported to the ocean increased” (page 11, line 4-5).

We have included the possible provenance of TAR:

“High TAR values can be indicative of relative increases in terrigenous organic matter transported to the ocean and/or to relative decreases in aquatic microorganism production. The opposite could explain low TAR values. To disentangle the old organic matter contamination from the fresh signal, we include the CPI index (Bray and Evans, 1961). High CPI values indicate a fresher or relatively newly produced organic matter transported to the ocean. CPI close to 1 indicate mature or old organic matter sources, such as coal or oil deposits, eroded to the ocean. This distinction may be important in the GOA, where the onshore bedrock includes units with high contents of terrigenous organic matter (e.g. the Yakutat Terrain, Childress, 2016; Walinsky *et al*., 2009).” (Page 5, lines 10-16).

We have included the CPI (carbon preference index) in Fig. 2 to help in visualising the diversity of material (indicated by the maturity of the sediments) reaching Site U1417 and thus, the diverse provenance of material eroded and transported to Site U1417.

1-Comment from the referee
Fourth, I would greatly reduce to just cut the discussion of the PDO or analogues to modern SST patterns from the paper. The whole section is very confusing and hard to follow. Likewise, this depends highly on the age models of all the cores and these are not discussed. To make such comparisons/conclusions, common age models and uncertainties need to be applied which I think is beyond the scope of this paper. Rather, the authors should smooth down to âG˘a˘0.1 Ma their records in Fig. 3 and support the idea that the North Pacific warmed over the Plio-Pleisto transition while the North Atlantic cooled. At the multi-0.1 Ma timescale, such a conclusion should be robust without delving into age models too far.

2-Author’s response
Both reviewers have commented on the complexity of this section and we agree that smoothing the data in Figure 3 of the manuscript and trim the text significantly would result in a clearer description of the North Pacific Plio-Pleistocene climate patterns.

3-Author’s changes in the revised manuscript
We have smoothed the data in Figure 3 of the manuscript to highlight more clearly the North Pacific Plio-Pleistocene climate patterns.

The text in section 4.4, has been edited (shortened and clarified) to read as follows:

“The overall cooling trend during the Neogene, briefly interrupted by the MPWP and intense cooling events such as the M2, is believed to be a dominant pattern in the global climate. This notion is largely based on the global increase in ice volume (e.g. LR04 Benthic δ^{18}O Stack (Lisiecki and Raymo, 2005) and from studies in the North Atlantic SST (i.e. ODP Site 982, Lawrence *et al*., 2009). In contrast, the contribution of the North Pacific into our understanding of the global climate evolution from the Pliocene to the Pleistocene is limited. Our study at Site U1417 adds valuable regional climate information during the evolution of the Cordilleran Ice Sheet. Unlike the LR04 stack, average Pliocene SST values (4.0 to 2.8 Ma) at Site U1417 are 1 °C colder than the average early Pleistocene values (2.7 to 1.7 Ma) (the Pliocene-Pleistocene SST difference of 1°C has an standard deviation of 0.5°C). In the wider North Pacific, a warming trend from the late Pliocene to early Pleistocene has also been observed at ODP Site 882 in the subarctic Pacific (Martínez-García *et al*., 2010), at Site 1010 and potentially at Site 1021 (mid-latitude east Pacific) (Fig. 3). Beyond the North Pacific, warmer SST during the early Pleistocene compared to the Pliocene have also been recorded i.e. DSDP Site 593 in the Tasman Sea (McClymont *et al*., 2016) and Site 1090 (Martínez-García *et al*., 2010) in the South Atlantic. In contrast, long-term cooling trends mark the early Pleistocene for the mid-latitude west Pacific (Site 1208) and tropical east Pacific (Site 846), more consistent with the development of a cooler and/or more glaciated climate (Fig. 3).

The North Pacific warming occurs despite an atmospheric CO_2 drop from 280-450 ppmv to 250-300 ppmv (similar to pre-industrial levels) from 3.2 to 2.8 Ma (Pagani *et al*., 2010; Seki *et al*., 2010) and an associated reduction in global radiative forcing (Foster *et al*., 2017). The early Pleistocene warming signal in the GOA (and the north Pacific more generally) thus implies an important role for local or regional processes. We have discussed above the potential role played by ocean stratification in the North Pacific, and a possible link to the evolving Cordilleran Ice Sheet in the GOA through evaporation/precipitation feedbacks. The synchrony of these changes with observed tectonic uplift (e.g. Enkelmann *et al*. 2015) makes it difficult to disentangle the potential climatic and tectonic mechanisms behind ice sheet expansion.

To understand the evolution of the ocean currents governing the North Pacific at the present core sites (Fig. 1) and to find possible explanations of the observed SST distributions during the Pliocene and Pleistocene climate evolution, the modern climate system is used here as an analogue. Modern monthly mean SSTs at ODP 882 SSTs are colder than Sites U1417 and 1021 all year around. During the late Pliocene and early Pleistocene, ODP 882 SSTs are 3-4 °C warmer than in the east (Fig. 3f and g). Modern seasonal climate analogues cannot be used to explain to Pliocene and Pleistocene subarctic SST distribution. However, on longer timescales, the strength of the AL is currently linked to the wider Pacific

Ocean circulation by the Pacific Decadal Oscillation (PDO) over periods of 20-30 years (Furtado *et al*., 2011). The Pliocene-Pleistocene North Pacific SST gradients show similarities with the negative phase of the PDO (-PDO), which is characterized by positive SST anomalies in the central North Pacific surrounded by negative SST anomalies along the North American coast and in the east equatorial Pacific. The -PDO associated route of winds might have increased the precipitation in the Gulf of Alaska and represent a key factor for the fast building of ice in the Alaskan mountains." (Page 13 and page 14).

1-Comment from the referee
In general, the paper needs some heavy editing on the writing side for clarity and grammar. For instance, conjunctions, such as "aren't", are used at points.

2-Author's response
Thank you.

3-Author's changes in the manuscript
We have carefully reviewed the manuscript to remove typos and improve the clarity in writing.

References cited in our reply:

Davies, M.H., Mix, A.C., Stoner, J.S., Addison, J.A., Jaeger, J., Finney. B., and Wiest, J. The deglacial transition of the southeastern Alaska Margin: Meltwater input, sea level rise, marine productivity, and sedimentary anoxia. Paleoceanography, Vol. 26, PA2223, 2011.

Jaeger, J.M., Gulick, S.P.S., LeVay, L.J., Asahi, H., Bahlburg, H., Belanger, C.L., Berbel, G.B.B., Childress, L.B., Cowan, E.A., Drab, L., Forwick, M., Fukumura, A., Ge, S., Gupta, S.M., Kioka, A., Konno, S., März, C.E., Matsuzaki, K.M., McClymont, E.L., Mix, A.C., Moy, C.M., Müller, J., Nakamura, A., Ojima, T., Ridgway, K.D., Rodrigues Ribeiro, F., Romero, O.E., Slagle, A.L.,Stoner, J.S., St-Onge, G., Suto, I., Walczak, M.H., and Worthington, L.L., 2014. Site U1417. In Jaeger, J.M., Gulick, S.P.S., LeVay, L.J., and the Expedition 341 Scientists, Proc. IODP, 341: College Station, TX (Integrated Ocean Drilling Program). doi:10.2204/iodp.proc.341.103.2014

Molnia, B.F., 2007. Late nineteenth to early twenty-first century behavior of Alaskan glaciers as indicators of changing regional climate. Global and Planetary Change, v. 56, p. 23-56.

Molnia, B.F., 2008. Glaciers of North America – Glaciers of Alaska: US Geological Survey Professional Paper 1386-K, 525 p.

Prueher, Libby M; Rea, David K: (Table 1) Age, magnetic susceptibility, and mass accumulation rate of volcanic glass and IRD from ODP Site 145-887. PANGAEA, https://doi.org/10.1594/PANGAEA.706309, 2001.

Scharman, R. M., Pavlis, T., Day, E & O'Driscoll, L. (2011). Deformation and structure in the Chugach metamorphic complex, southern Alaska: Crustal architecture of a trans- pressional system from a down plunge section. Geosphere. 10. 10.1130/GES00646.1.

St. John, K.E.K and Krissek, L.A., Regional patterns of Pleistocene ice-rafted debris flux in the North Pacific. Paleoceanography, Vol. 14, 653-662, 1999.
Weingartner, T.J., Danielson, S.L. and Royer, T.C., 2005, Freshwater variability and predictability in the Alaska Coastal Current, Deep-Sea Research Part II-Topical Studies in Oceanography, 52 (1-2): 169-191.
Royer, T. C. and Grosch, C. E., 2006, Ocean Warming and freshening in the northern Gulf of Alaska, Geophysical Research Letters, Vol. 33, L16605, doi:10.1029/2006GL026767, 2006.

Interactive comment on Clim. Past Discuss., https://doi.org/10.5194/cp-2019-29, 2019.

We would like to thank Anonymous Referee 2 for the constructive comments provided to help us improve our manuscript. Please find below our responses to these comments and the manuscript changes.

1-Comment from Referee
Sánchez-Montes et al. present a new comprehensive set of Plio-Pleistocene records from IODP site U1417 in the Gulf of Alaska encompassing SST, IRD, input of terrigenous organic matter and pollen counts. The authors infer dynamics of the Cordilleran ice sheet over 4-1.7 Ma and discuss conceptual models for potential climatic controls. It is an exciting dataset and a valuable contribution to the debate on regional versus global climatic triggers for glaciation in the Northeast-Pacific realm during the Northern Hemisphere Glaciation. The study also adds new information to the plioVar database. The application of biomarkers, pollen and IRD is robust and state of the art. Nevertheless, the manuscript needs some revision regarding the clarity and logic of several parts in the discussion. The interpretations of the TAR-index partly need a more detailed discussion to clarify the interactions of different factors controlling the TAR (i.e. vegetation cover, petrogenic contributions and aquatic production) and the link to glaciation. At the present stage, particularly section 4.3 on the iNHG and the early Pleistocene is inconclusive with respect to variations in the sources of organic matter and the inferences on glaciation dynamics in the region. Also, the chronology of processes described in section 4.3 is a bit convoluted. In order to clarify and strengthen the interpretations of the TAR-index, the CPI has to be better represented in the manuscript. At the moment it is mentioned a few times in the text but the record is not shown in any figure. I recommend to plot the CPI along with the TAR in figure 2.

2-Author's response
We agree that adding a more detail discussion on the TAR sources and associations with climate would help to deliver a clearer message in our manuscript. We will include details as suggested (see replies on your detailed comments at the end of the document). The authors agree that including the CPI record in Fig. 2 in the manuscript would help in visualising its variations, including arrows where organic matter becomes more/less mature. We will amend Fig. 2 to include the CPI and we will present some information on the broad changes in organic matter sources to the GOA (since the data shows a slight increase towards less mature OM as IRD inputs increase). As the reviewer notes (and as we noted in our reply to reviewer 1), there are multiple potential sources to the TAR, including complex onshore petrogenic sources (Yakutat terrain; Childress, 2016), which are not easily disentangled. In the revised manuscript we can comment that we see evidence for less mature organic matter (increase in CPI) contributing as ice-rafting increases and the TAR decreases, suggesting a potential shift in organic matter source as the glaciation develops.

3-Author's changes in the revised manuscript
We have amended Fig. 2 to include the CPI and have included some information on the broad changes in organic matter sources to the GOA and ways to explain them in:

"Terrigenous and aquatic organic matter sources increase during the early Pleistocene in comparison with the late Pliocene. High TAR values can be indicative of relative increases in terrigenous organic matter transported to the ocean and/or to relative decreases in aquatic microorganism production. The opposite could explain low TAR values. To disentangle the old organic matter contamination from the fresh signal, we include the CPI index (Bray and Evans, 1961). High CPI values indicate a fresher or relatively newly produced organic matter transported to the ocean. CPI close to 1 indicate mature or old organic matter sources, such as coal or oil deposits, eroded to the ocean. This distinction may be important in the GOA, where the onshore bedrock includes units with high contents of terrigenous organic matter (e.g. the Yakutat Terrain, Childress, 2016; Walinsky *et al*., 2009).” (Page 5, lines 9-16)

and links to glaciation

”the TAR and CPI values at Site U1417 thus suggest a mix of sources of organic matter during this time dominated by contemporaneous vegetation, although we cannot exclude the possibility of some coal erosion." (absent/limited glaciation) Page 10, lines 29-31.

“From 3 Ma, TAR values decrease to below the average of the entire TAR record, indicating that transport of leaf-wax lipids to Site U1417 increased in comparison with the Pliocene, which may be related to an increase in erosion on land due to the advancing ice-sheet.” (Page 10, lines 40-41 and Page 11 line 1).

“ The most reasonable explanation is that the land was becoming increasingly ice covered, so that the erosion of vegetation and terrigenous organic matter eroded and transported to the ocean increased.”(page 11, lines 4-5)

“The CPI values discard mature sources of organic matter to the GOA at this time interval suggesting a contemporary aquatic organic matter contribution.” (Page 12 lines 10-13).

“An additional explanation for the changing TAR during the early Pleistocene is that tectonic uplift of the Chugach/St Elias area from 2.7 Ma (Enkelmann *et al*., 2015) led to orogenic precipitation and a change in erosional pathways (Enkelmann *et al*., 2015). The glaciation could have altered the main source of terrestrial input to the Surveyor Channel, to higher metamorphic and plutonic sources with lower or null TAR values (Childress, 2016). An increase in CPI variability to concentrations up to 2 and 3 during the early Pleistocene (starting from 2.7 Ma) supports the change of source of organic matter away from the more mature coal bedrock into more immature terrestrial organic matter (plant waxes). However, this comes at a time of increasing IRD, which adds a new source of terrigenous sediment to Site 1417. The shift in CPI values at 2.7 Ma agrees with the shift towards the erosion of sediments sourced from metamorphic and plutonic sources, described in Enkelmann et al. (2015) delivered to Site U1417.” (Page 12 lines 23-31).

1-Comment from Referee
In section 4.4 the discussion about the climatic controls on glaciation is very hard to follow and needs to be revisited for clarity. The reader gets lost in the detailed descriptions and comparisons of different gradients during the Plio-Pleistocene and today. I recommend to at least shorten these paragraphs or to

delete them. Similarly, the extensive discussion of the PDO analogue in cold and warm periods is confusing and could be shortened. Since the Plio-Pleistocene SST gradients are highly dependent to uncertainties in the absolute SST-estimates associated with the application of UK'37, the gradients need to be discussed in context of those uncertainties. In light of uncertainties on absolute values, section 4.4 would be strengthened by setting the focus on the warming trend that is recorded across the entire North Pacific instead of setting it on the SST gradients.

2-Author's response
This was also a concern of Reviewer 1. The authors agree that this section needs to be shortened to avoid complexity.

3-Author's changes in the revised manuscript
We have implemented your comments and edit this section accordingly. In addition, we have smoothed down to 100 kyr the data sets in Figure 3 in the manuscript following Reviewer 1's advice.

The text in section 4.4 has been edited (shortened and clarified) to read as follows:

"The overall cooling trend during the Neogene, briefly interrupted by the MPWP and intense cooling events such as the M2, is believed to be a dominant pattern in the global climate. This notion is largely based on the global increase in ice volume (e.g. LR04 Benthic δ^{18}O Stack (Lisiecki and Raymo, 2005) and from studies in the North Atlantic SST (i.e. ODP Site 982, Lawrence *et al*., 2009). In contrast, the contribution of the North Pacific into our understanding of the global climate evolution from the Pliocene to the Pleistocene is limited. Our study at Site U1417 adds valuable regional climate information during the evolution of the Cordilleran Ice Sheet. Unlike the LR04 stack, average Pliocene SST values (4.0 to 2.8 Ma) at Site U1417 are 1 °C colder than the average early Pleistocene values (2.7 to 1.7 Ma) (the Pliocene-Pleistocene SST difference of 1°C has an standard deviation of 0.5°C). In the wider North Pacific, a warming trend from the late Pliocene to early Pleistocene has also been observed at ODP Site 882 in the subarctic Pacific (Martínez-García *et al*., 2010), at Site 1010 and potentially at Site 1021 (mid-latitude east Pacific) (Fig. 3). Beyond the North Pacific, warmer SST during the early Pleistocene compared to the Pliocene have also been recorded i.e. DSDP Site 593 in the Tasman Sea (McClymont *et al*., 2016) and Site 1090 (Martínez-García *et al*., 2010) in the South Atlantic. In contrast, long-term cooling trends mark the early Pleistocene for the mid-latitude west Pacific (Site 1208) and tropical east Pacific (Site 846), more consistent with the development of a cooler and/or more glaciated climate (Fig. 3).

The North Pacific warming occurs despite an atmospheric CO_2 drop from 280-450 ppmv to 250-300 ppmv (similar to pre-industrial levels) from 3.2 to 2.8 Ma (Pagani *et al*., 2010; Seki *et al*., 2010) and an associated reduction in global radiative forcing (Foster *et al*., 2017). The early Pleistocene warming signal in the GOA (and the north Pacific more generally) thus implies an important role for local or regional processes. We have discussed above the potential role played by ocean stratification in the North Pacific, and a possible link to the evolving Cordilleran Ice Sheet in the GOA through evaporation/precipitation feedbacks. The synchrony of these changes with observed tectonic uplift (e.g. Enkelmann *et al*. 2015) makes it difficult to disentangle the potential climatic and tectonic mechanisms behind ice sheet expansion.

To understand the evolution of the ocean currents governing the North Pacific at the present core sites (Fig. 1) and to find possible explanations of the observed SST distributions during the Pliocene and Pleistocene climate evolution, the modern climate system is used here as an analogue. Modern monthly mean SSTs at ODP 882 SSTs are colder than Sites U1417 and 1021 all year around. During the late Pliocene and early Pleistocene, ODP 882 SSTs are 3-4 °C warmer than in the east (Fig. 3f and g). Modern seasonal climate analogues cannot be used to explain to Pliocene and Pleistocene subarctic SST distribution. However, on longer timescales, the strength of the AL is currently linked to the wider Pacific Ocean circulation by the Pacific Decadal Oscillation (PDO) over periods of 20-30 years (Furtado *et al*., 2011). The Pliocene-Pleistocene North Pacific SST gradients show similarities with the negative phase of the PDO (-PDO), which is characterized by positive SST anomalies in the central North Pacific surrounded by negative SST anomalies along the North American coast and in the east equatorial Pacific. The -PDO associated route of winds might have increased the precipitation in the Gulf of Alaska and represent a key factor for the fast building of ice in the Alaskan mountains." (Page 13 and page 14).

1-Comment from Referee
Moreover, the manuscript should be revisited in terms of language and grammar. There are several spelling and grammar mistakes throughout the manuscript (see detailed comments below). This also applies to the supplementary material.

2-Author's response
Thank you.

3-Author's changes in the revised manuscript
We have reviewed the manuscript for typos and amend the ones that you highlight below.

1-Comment from Referee
p. 1, line 24: MPWP should be called Mid-Piacenzian-Warm-Period.

2-Author's response and 3- Changes in the revised manuscript
We have changed this in page 1, line 24.

1-Comment from Referee
p. 5, line 19: ". . .provides similar SST estimates in northern high latitudes than previous calibrations." Replace "than" by "to".

2-Author's response and 3-Author's changes in the revised manuscript

We have changed this in page 5 line 33.

1-Comment from Referee
p. 5, lines 17-20. I recommend to mention the standard errors of the calibrations.

2-Author's response and 3-Author's changes in the revised manuscript
We have mentioned this

"which accuracy is constrained by an standard error of ±1.5 ◦C" (Page 5 lines 31-32)

"The standard error of Prahl et al. (1988) (Eq. (4)) is ±1.0 ◦C". (Page 6 line 3-4).

1-Comment from Referee
p.5, line 23: It would be helpful for non-biomarker experts to indicate what the authors wish to reconstruct using the %C37:4.

2-Author's response and 3-Author's changes in the revised manuscript
We have explained the C37:4 previous interpretations:

"The %$C_{37:4}$ represents fresher and cooler surface water characteristics (Bendle *et al*., 2005). In the Nordic Seas this has been linked to subpolar and polar water masses (Bendle *et al.,* 2005), whereas elsewhere in the North Atlantic it has been linked to freshwater inputs (e.g. during Heinrich events, Martrat *et al.*, 2007). In the subarctic Pacific, the %$C_{37:4}$ proxy has been less well studied (McClymont *et al*., 2008), but high %$C_{37:4}$ is also proposed to reflect cooler and fresher water masses (Harada *et al*., 2006)." (Page 6 lines 5-9).

And later we interpret it as glacier meltwater sourced at Site U1417:

"%$C_{37:4}$ increases can be related to colder sea surface conditions, but due to Site U1417's location and climatic context, we suggest that increases in %$C_{37:4}$ relate to meltwater discharge from the expanding ice-sheet." (Page 10 lines 35-37).

1-Comment from Referee
p.5, line 29: Sentence uses present tense. Turn to simple past.

2-Author's response and 3-Author's changes in the revised manuscript
We have changed this in page 6 line 14.

1-Comment from Referee
p. 7, line 1: What is the standard deviation of the statistical mean?

2-Author's response and 3-Author's changes in the revised manuscript
We have included this value in the revised manuscript in page 7 line 18.

1-Comment from Referee
p. 7, line 5: "Gi1 period (3.6-3.4 Ma) warm period. . .": I suggest to write . . ."Gi1 warm period (3.6-3.4 Ma)" or something similar along this line.

2-Author's response and 3-Author's changes in the revised manuscript
We have changed this in page 7 line 23.

1-Comment from Referee
p. 7 lines 22-24: It is not clear how the high TAR-values relate to limited mountain glaciation as the interpretation of the TAR is missing. The same applies to the %C37:4.

2-Author's response and 3-Author's changes in the revised manuscript
We have explained the interpretation of TAR:

"Terrigenous and aquatic organic matter sources increase during the early Pleistocene in comparison with the late Pliocene. High TAR values can be indicative of relative increases in terrigenous organic matter transported to the ocean and/or to relative decreases in aquatic microorganism production. The opposite could explain low TAR values. To disentangle the old organic matter contamination from the fresh signal, we include the CPI index (Bray and Evans, 1961). High CPI values indicate a fresher or relatively newly produced organic matter transported to the ocean. CPI close to 1 indicate mature or old organic matter sources, such as coal or oil deposits, eroded to the ocean. This distinction may be important in the GOA, where the onshore bedrock includes units with high contents of terrigenous organic matter (e.g. the Yakutat Terrain, Childress, 2016; Walinsky *et al*., 2009)." (Page 5 lines 9-16).

We have amended Fig. 2 to include the CPI.

We have included some information on the broad changes in organic matter sources to the GOA:

"Terrigenous and aquatic organic matter sources increase during the early Pleistocene in comparison with the late Pliocene. High TAR values can be indicative of relative increases in terrigenous organic matter transported to the ocean and/or to relative decreases in aquatic microorganism production. The opposite could explain low TAR values. To disentangle the old organic matter contamination from the fresh signal, we include the CPI index (Bray and Evans, 1961). High CPI values indicate a fresher or relatively newly produced organic matter transported to the ocean. CPI close to 1 indicate mature or old organic matter sources, such as coal or oil deposits, eroded to the ocean. This distinction may be important in the GOA, where the onshore bedrock includes units with high contents of terrigenous organic matter (e.g. the Yakutat Terrain, Childress, 2016; Walinsky *et al*., 2009).” (Page 5, lines 9-16).

and links to glaciation:

“the TAR and CPI values at Site U1417 thus suggest a mix of sources of organic matter during this time dominated by contemporaneous vegetation, although we cannot exclude the possibility of some coal erosion.” (absence/limited glaciation) (Page 10 lines 29-31)

“From 3 Ma, TAR values decrease to below the average of the entire TAR record, indicating that transport of leaf-wax lipids to Site U1417 increased in comparison with the Pliocene, which may be related to an increase in erosion on land due to the advancing ice-sheet.” (Page 10 lines 40-41 and Page 11, line 1).

“The most reasonable explanation is that the land was becoming increasingly ice covered, so that the erosion of vegetation and terrigenous organic matter eroded and transported to the ocean increased.” (Page 11, lines 4-5).

“This could point to an increase in marine productivity export related to an enhanced nutrient delivery to Site U1417 via glacial runoff.” (Page 12 lines 11-12).

“An additional explanation for the changing TAR during the early Pleistocene is that tectonic uplift of the Chugach/St Elias area from 2.7 Ma (Enkelmann *et al*., 2015) led to orogenic precipitation and a change in erosional pathways (Enkelmann *et al*., 2015). The glaciation could have altered the main source of terrestrial input to the Surveyor Channel, to higher metamorphic and plutonic sources with lower or null TAR values (Childress, 2016). An increase in CPI variability to concentrations up to 2 and 3 during the early Pleistocene (starting from 2.7 Ma) supports the change of source of organic matter away from the more mature coal bedrock into more immature terrestrial organic matter (plant waxes). However, this comes at a time of increasing IRD, which adds a new source of terrigenous sediment to Site 1417. The shift in CPI values at 2.7 Ma agrees with the shift towards the erosion of sediments sourced from metamorphic and plutonic sources, described in Enkelmann et al. (2015) delivered to Site U1417. “ (Page 12, lines 23-31).

The C37:4 sources are explained now in:

“The %$C_{37:4}$ represents fresher and cooler surface water characteristics (Bendle *et al*., 2005). In the Nordic Seas this has been linked to subpolar and polar water masses (Bendle *et al.,* 2005), whereas elsewhere in the North Atlantic it has been linked to freshwater inputs (e.g. during Heinrich events, Martrat *et al.*, 2007). In the subarctic Pacific, the %$C_{37:4}$ proxy has been less well studied (McClymont *et al*., 2008), but high %$C_{37:4}$ is also proposed to reflect cooler and fresher water masses (Harada *et al*., 2006).” (Page 6, line 6-9) and its link to glaciation are included in:

"%$C_{37:4}$ increases can be related to colder sea surface conditions, but due to Site U1417's location and climatic context, we suggest that increases in %$C_{37:4}$ relate to meltwater discharge from the expanding ice-sheet." (Page 10, line 35-37).

"We attribute this 0.3 Ma progressive cooling to the oNHG in response to the overall decrease in the atmospheric CO_2 (Seki *et al.,* 2010; Martínez-Botí *et al*., 2015)." (Page 10, lines 38-39)

"The relatively high %$C_{37:4}$ (up to 24 %) in the early Pleistocene correlates well with the period of high IRD delivery (up to 4 g cm^{-2} Ka^{-1}) between 2.7 to 2.4 Ma (Fig. 2b and c). This suggests this period marks an expansion/intensification of the Cordilleran glaciation following a gradual SST cooling during the oNHG." (Page 11, line 23-25).

1-Comment from Referee
p. 11, lines 1-3: What about petrogenic contributions?

2-Author's response and 3-Author's changes in the revised manuscript

We have included references to petrogenic contributions in:

"the TAR and CPI values at Site U1417 thus suggest a mix of sources of organic matter during this time dominated by contemporaneous vegetation, although we cannot exclude the possibility of some coal erosion." (Page 10, line 29-31).

"The CPI values discard mature sources of organic matter to the GOA at this time interval suggesting a contemporary aquatic organic matter contribution." (Page 12 lines 12-13).

1-Comment from Referee
p. 11, line 7: Which interval is meant by: "at first"?

2-Author's response and 3-Author's changes in the revised manuscript
We have changed this to read:

"This could indicate that the first IRD in icebergs delivered to the GOA during the late Pliocene and early Pleistocene originated from smaller marine terminating valley glaciers which removed sediment and weathered rock from the landscape rather than eroding bedrock and allowed IRD generation." (Page 12, line 17-20).

1-Comment from Referee
p. 11, line 9: How does the erosion pattern explain the TAR? I don't understand which TAR-variations the authors address.

2-Author's response and 3-Author's changes in the revised manuscript
We have deleted this sentence as the idea is better expressed in the previous sentence (see previous comment) and in: "The most reasonable explanation is that the land was becoming increasingly ice covered, so that the erosion of vegetation and terrigenous organic matter eroded and transported to the ocean increased." (Page 11, lines 4-5).

1-Comment from Referee
p. 11, line 12: Do the authors mean an "alternative or additional explanation" to the interpretations in lines 1-3?

2-Author's response and 3-Author's changes in the revised manuscript
This have now changed this to read "Additional" only in page 12 line 23.

1-Comment from Referee
p. 11, lines 12-15: which changes in the TAR do the authors mean? Do they refer to the iNHG or the period afterwards? Does the CPI record a change in the source?

2-Author's response and 3-Author's changes in the revised manuscript
We have made this clearer by adding a time reference in the sentence:

"An additional explanation for the changing TAR during the early Pleistocene is that tectonic uplift of the Chugach/St Elias area from 2.7 Ma (Enkelmann et al., 2015) led to orogenic precipitation and a change in erosional pathways (Enkelmann et al., 2015)." (Page 12 lines 24-25).

Then this sentence link to the CPI values mentioned in the next sentence over the same time period.

1-Comment from Referee
p.11, lines 16-17: when exactly is this change in the CPI recorded? How is the switch in the source "away from the more mature coal bedrock" connected to the Surveyor Channel? Does it mark a switch to the channel or a switch away from the channel?

2-Author's response and 3-Author's changes in the revised manuscript

Site U1417, which is located in the surveyor Channel, contains organic matter with a different provenance: terrigenous from different sources (vegetation and different land sediments or aquatic (i.e. phytoplankton). We have made changes to include:

“An increase in CPI variability to concentrations up to 2 and 3 during the early Pleistocene (starting from 2.7 Ma) supports the change of source of organic matter away from the more mature coal bedrock into more immature terrestrial organic matter (plant waxes). However, this comes at a time of increasing IRD, which adds a new source of terrigenous sediment to Site 1417. The shift in CPI values at 2.7 Ma agrees with the shift towards the erosion of sediments sourced from metamorphic and plutonic sources, described in Enkelmann et al. (2015) delivered to Site U1417.” (Page 12, lines 26-31).

1-Comment from Referee
p. 11, lines 20-21: I recommend to add a standard deviation to the average values.

2-Author’s response and 3-Author’s changes in the revised manuscript
We have included this number:

“(the Pliocene-Pleistocene SST difference of 1°C has an standard deviation of 0.5°C)” (Page 13 lines 7-8).

1-Comment from Referee
p. 13, line 9: decree or degree?

2-Author’s response and 3-Author’s changes in the revised manuscript
We have now erased this sentence as part of the shortening of section 4.4 requested.

1-Comment from Referee
p. 13, line 10: “aren’t” should be “are not”.

2-Author’s response and 3-Author’s changes in the revised manuscript
We have now erased this sentence as part of the shortening of section 4.4 requested.

1-Comment from Referee
p.13, lines 11-13: the reference to the figures seems to be mixed up here. C is indicated as summer in the text while in figure 1 panel C is references as winter.

2-Author’s response and 3-Author’s changes in the revised manuscript
We have now erased this sentence as part of the shortening of section 4.4 requested.

1-Comment from Referee
p.14, lines 21-22: how do the vegetation reconstructions from this study fit the results deduced from the El'Gygytgyn pollen record?

2-Author's response and 3-Author's changes in the revised manuscript
We have deleted this reference during the shortening of section 4.4 requested.

1-Comment from Referee
p.14, line 32, "the data is the first climatic data": replace "is" by "are".

2-Author's response and 3-Author's changes in the revised manuscript
We have now erased this sentence as part of the shortening of section 4.4 requested.

1-Comment from Referee
Figure 1: The sites can be larger and I also suggest to add the study site U1417 to panel A.

2-Author's response and 3-Author's changes in the revised manuscript
We have changed this in Fig. 1.

1-Comment from Referee
Figure 2 and 3: I recommend to increase the size of these figures. They show a lot of data and the small size makes them look quite busy. It is sometimes hard to read the small annotations. I suggest to increase the font size and also the lengths of the x-axes. Some graphs overlap each other as the y-axes are very closely spaced. The distances between the y-axes should be increased a bit. The x-axes would be easier to read if minor ticks were shown. In Figure 3 the line thickness of the x-axis should be increased and I suggest to add data points to the single graphs, as done in Figure 2.

2-Author's response and 3- Changes in manuscript
We have edited this in Fig. 2 and 3.

References cited in our reply:
Addison, J., A., Finney, B. P., Dean, W. E., Davies, M. H., Mix, A. C., Stoner, J. S. and Jaeger, J. M., 2012, Productivity and sedimentary d15N variability for the last 17,000 years along the northern Gulf of Alaska continental slope, Paleoceanography, Vol 27, PA 1206.

Childress, L. B., 2016, The Active Margin Carbon Cycle: Influences of Climate and Tectonics in Variable Spatial and Temporal Records, PhD thesis Northwestern University, Evanson, Illinois.

Interactive comment on Clim. Past Discuss., https://doi.org/10.5194/cp-2019-29, 2019.

Fig. 1. Figure 1 TAR, CPI, SR and IRD at Site U1417. Missing data points are either a result of samples analysed for SSTs at the early stages of the project which were not subsequently analysed for n-alkanes.
Fig. 2. Figure 2: ∼100 Kyr smoothed North Pacific sites (adapted from Fig. 3 in original manuscript).
Fig. 3. Table 1: N/C vs δ13C (‰) at Site U1417 vs range of data at EW0408–85JC (Addison et al., 2012). Data from the Pliocene (4 to 3 Ma), NHG (2.9 to 2.4 Ma) and the early Pleistocene (2.3-1.7 Ma).

Late Pliocene Cordilleran Ice Sheet development with warm Northeast Pacific sea surface temperatures

Maria Luisa Sánchez-Montes[1], Erin L. McClymont[1], Jeremy M. Lloyd[1], Juliane Müller[2], Ellen A. Cowan[3] and Coralie Zorzi[4].

[1] Geography Department, Durham University, Durham, DH1 3LE, UK.
[2] Alfred Wegener Institute, Helmholtz Centre for Polar and Marine Research, Bremerhaven, 27568, Germany.
[3] Department of Geological and Environmental Sciences, Appalachian State University, North Carolina, 28608, USA.
[4] GEOTOP, Université du Québec à Montréal, Montreal, H3C 3P8, Canada.

Correspondence to: Maria Luisa Sánchez Montes (m.l.sanchez-montes@durham.ac.uk)

Abstract. The initiation and evolution of the Cordilleran Ice Sheet is relatively poorly constrained. International Ocean Discovery Program (IODP) Expedition 341 recovered marine sediments at Site U1417 in the Gulf of Alaska (GOA). Here we present alkenone-derived sea surface temperature (SST) analyses alongside ice rafted debris (IRD), terrigenous and marine organic matter inputs to the GOA through the late Pliocene and early Pleistocene. The first IRD contribution from tidewater glaciers in southwest Alaska is recorded at 2.9 Ma, indicating that the Cordilleran ice sheet extent increased in the late Pliocene. A higher occurrence of IRD and higher sedimentation rates in the GOA during the early Pleistocene, at 2.5 Ma, occur in synchrony with SSTs warming on the order of 1°C relative to the Pliocene. All records show a high degree of variability in the early Pleistocene, indicating highly efficient ocean-climate-ice interactions through warm SST-ocean evaporation-orographic precipitation-ice growth mechanisms. A climatic shift towards ocean circulation in the subarctic Pacific similar to the pattern observed during negative Pacific Decadal Oscillation (PDO) conditions today appears to be a necessary pre-requisite to develop the Cordilleran glaciation and increase moisture supply to the subarctic Pacific. The drop in atmospheric CO_2 concentrations since 2.8 Ma is suggested as one of the main forcing mechanisms driving the Cordilleran glaciation.

1 Introduction

During the Neogene, the global climate transitioned from relatively warm to cooler conditions that enabled the development of ice masses in both hemispheres (Zachos *et al*., 2001a). The Mid-Piacenzian Warm Period (MPWP, 3.3-3.0 Ma) interrupts this cooling trend, with global temperatures around 2-3 °C above pre-industrial levels (Jansen *et al*., 2007; Haywood *et al*., 2004), and more intense warming at higher latitudes (Haywood *et al*., 2013; Dolan *et al*., 2015). The MPWP has been suggested as a potential analogue for the 21st century climate due to the atmospheric CO_2 concentrations (400 ppmv) and largely equivalent continental configurations relative to the present (Salzmann *et al*., 2011; Raymo *et al*., 1996, Jansen *et al*., 2007). Overall, the mid-Pliocene ice masses were smaller than today (Dolan *et al*., 2011). However, the marine isotope stage (MIS) M2 (~3.3-3.26 Ma) event is characterised by a dramatic cooling in the Atlantic Ocean and is considered to be an unsuccessful attempt at a glaciation (De Schepper *et al*., 2013). The later onset (oNHG) or intensification (iNHG) of the Northern

Deleted: Pliocene

Hemisphere Glaciation is marked by the expansion of the Laurentide, Greenland and Scandinavian ice sheets around 2.5 Ma indicated by ice rafted debris (IRD) records from the North Atlantic Ocean (i.e. Shackleton *et al*., 1984) and the advance of the Cordilleran Ice Sheet at 2.7 Ma inferred from a terrestrial record (Hidy *et al*., 2013). It is still debated whether climatic or tectonic forcing was the main driver of the North Hemisphere Glaciation (NHG) (Haug *et al*., 2005), as it cannot be explained solely by changes in isolation (Lunt *et al*., 2008). The decrease in atmospheric CO_2 concentrations and radiative forcing at 2.8 Ma has been identified as a potential mechanism for climate cooling of the oNHG (Seki *et al*., 2010; Martínez-Botí *et al*., 2015). However, the timing of the oNHG varies between locations based on IRD delivery, and at some locations the NHG has been set as far back as 3.5 Ma (Nordic Seas, Mudelsee and Raymo, 2005). Alternative proposals for the oNHG suggest that orogenic changes could have led to an increase in heat transport to the North Atlantic region during the Pliocene potentially increasing precipitation in higher latitudes promoting glacial development during the Plio-Pleistocene transition (Sarnthein *et al*, 2013; Haug *et al*., 2005; Bringham-Grette *et al.,* 2013; Fedorov *et al.,* 2013; Lawrence *et al.,* 2010).

It remains unclear whether the Cordilleran Ice Sheet of North America expanded across the oNHG, although enhanced delivery of terrigenous sediments to the Gulf of Alaska (GOA; Northeast Pacific Ocean) since 2.7 Ma has been interpreted as evidence for ice sheet growth (Gulick *et al*., 2014). The sediments of the Gulf of Alaska (GOA) record Cordilleran glaciation in the St. Elias Mountains, at present the highest coastal mountain range in the world (Enkelmann *et al*., 2015). It has been proposed that the uplift of the St. Elias Range from early Pliocene to early Pleistocene led to an increase in orographic precipitation and subsequent increase in sedimentation rates in the GOA (Enkelmann *et al*., 2015). Mountain glaciation may have developed in the St Elias mountains as early as 5.5 Ma (Reece *et al*., 2011), ultimately developing tidewater glaciers, with the high erosion pathway shifting to the southern St Elias Range at 2.6 Ma (Enkelmann *et al*., 2015). Rather than a tectonic control on Cordilleran glaciation, an alternative explanation could be the reduced radiative forcing and climate cooling associated with the decline in CO_2 at 2.8 Ma. However, it is difficult to resolve these hypotheses in the absence of high resolution data for both ice sheet extent and climate from the GOA. Despite the global drop in atmospheric CO_2 at 2.8 Ma, it remains unclear whether the Cordilleran Ice Sheet also expanded.

Here, we present a new multiproxy data set obtained from IODP core site U1417 (56° 57.58' N, 147° 6.58' W, water depth 4218 m; Fig. 1) in the GOA. The core site allows examination of the land-ocean interactions associated with advance and retreat phases of the Cordilleran Ice Sheet across the Pliocene-Pleistocene transition, in the context of mountain uplift. The sediments were collected during IODP Expedition 341 (Jaeger *et al.,* 2014) and were analysed to reconstruct sea surface conditions by means of alkenone and IRD data covering the time interval from 4 to 1.7 Ma years ago. Terrestrial organic matter input to Site U1417 is assessed through the abundance of long-chain *n*-alkanes and palynological analysis.

2 Study area

2.1 The Gulf of Alaska (GOA)

Deleted: ,

Formatted: Not Highlight

Deleted: magnetic susceptibility measurements at ODP Site 882 in the northwest Pacific Ocean (Haug *et al*., 1999; Haug *et al*., 2005

The GOA extends from the Alaska Peninsula in the west to the Alexander Archipelago in the east (Hogan, 2013), delimited by the Bering Sea on the west and the Alaska coast in the north and east, which is, in turn, bounded to the north by the Pacific Mountain System (Molnia, 2008). The south of the GOA connects with the North Pacific Ocean (Fig. 1). Glaciers cover 20% of the Gulf of Alaska watershed (Spies, 2007), and the major rivers draining the St. Elias and Chugach mountains towards the GOA (the Alsek River and the Copper River), are fed by meltwater discharge which peaks in August (Weingartner, 2007). The GOA mean annual freshwater discharge derives from high precipitation, runoff and snow melt from watersheds along the SE Alaskan coast (Spies, 2007). High precipitation is due in part to the proximity of the North Pacific Ocean, as a source of moisture, and the high topography of the Pacific Mountain System driving orographic precipitation.

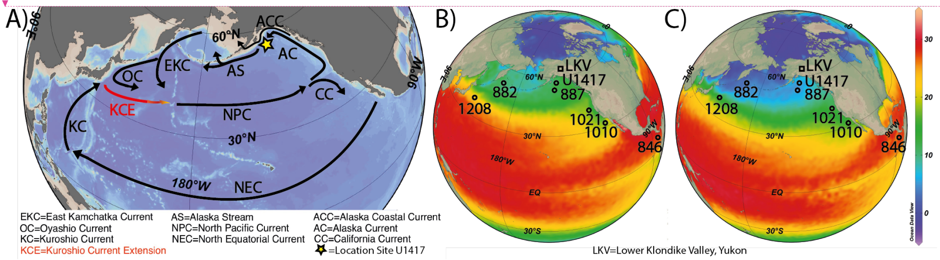

Figure 1: Map of modern ocean circulation and SSTs. a) Modern North Pacific Ocean circulation, b) September c) and December 1955-2013 SST average centred in the North Pacific Ocean (NOAA WOA13, Locarnini *et al*., 2013) and core and sample sites discussed in this study. Map made using Ocean Data View (Schlitzer, 2018).

Deleted:

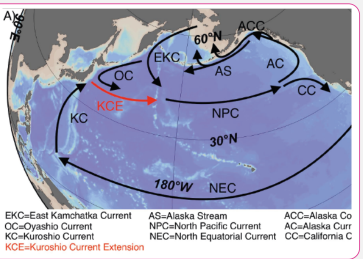

The Alaskan Coastal Current (ACC) flows anti-clockwise along the GOA coastline and westward to the Bering Sea (Fig. 1a), and its properties are dominated by nutrient and meltwater supply from the coastal Alaskan glaciers (Spies, 2007). Further offshore, the Alaska Current (AC) also flows anti-clockwise, controlled in strength by the Alaska Gyre (Kato *et al*., 2016) (Fig. 1a). The location of Site U1417 rests under the modern influence of the AC (Fig. 1). The Alaskan Gyre is, in turn, influenced by atmospheric circulation via the Aleutian Low (AL) and the Pacific High Pressure Systems, which are coupled in an annual cycle. High pressures dominate during the summer season and low pressures dominate during autumn to spring (Hogan, 2013), when the AL also migrates eastward across the North Pacific Ocean, becoming most intense when located in the GOA during winter (Pickart *et al.,* 2009). The coast of Alaska receives high winter precipitation because of the AL winter position and strength (Rodinov *et al.,* 2007) and Alaska's high topography which drives orographic precipitation. The GOA locally receives annual precipitation of ~800 cm (Powell and Molnia, 1989). During summer, the AL is less intense and almost disappears when it is located in the Bering Sea. A weaker AL is translated into reduced precipitation over the GOA.

A strong winter AL also creates a strong zonal SST gradient in the North Pacific Ocean (Fig. 1b). During winter, the ocean responds to a more intense AL through southward movement of the cold Arctic waters, and northward flow of mid-latitude warm waters into the Gulf of Alaska through the AC. During the summer migration of the AL northwards, the GOA registers higher SSTs due to higher insolation on the North Pacific Ocean, and as the zonal SST gradient is reduced, the storms diminish (Pickart *et al.,* 2009) (Fig. 1c).

3 Material and Methods

3.1 Age model and sedimentation rates

The shipboard age model was calculated using magnetostratigraphy (Jaeger *et al*., 2014, Fig. S1-3). The recovery of the Pliocene-early Pleistocene sediments averaged 70 % (Expedition 341 Scientists, 2014), with a number of core breaks in the record. Poor carbonate preservation across the Pliocene and early Pleistocene prevents the production of a higher resolution stable isotope stratigraphy. The shipboard depth models place all discrete core biscuits to the upper depth range of each core, and a continuous core break below; it is possible that the biscuits were originally distributed through the core barrel before recovery on the ship. We have converted the depth scale of our data sets to assume an even distribution of core biscuits and core breaks (Fig. S1), converted these depths to age and interpolated the ages of the samples between core top and bottom (Fig. 2 and Figs. S1-S3). The magnetostratigraphy ages were similar between the shipboard and new age model; The Gauss/Matuyama magnetic reversal (2.581 ±0.02 Ma and 330.76 ±1 m CCSF-A) was well constrained in multiple holes to provide an important age control point for this study (Fig. S1). The shipboard age model sedimentation rates show a marked but temporary increase between 2.5-2.0 Ma, which has been attributed to the first major erosion of the landscape by expansion of the Cordilleran Ice Sheet (Gulick *et al*., 2014). Our new sedimentation rates detail a two-step increase from 2.5-2.4 and from 2.4-2.0 Ma (Fig. S3).

3.2 Biomarkers

A total of 119 biomarker samples between 4 and 1.7 Ma were analysed for biomarkers, which corresponds to an average sampling resolution of 19 kyr. Microwave lipid biomarker extraction was carried out following the method of Kornilova and Rosell-Melé (2003). The total lipid extract was separated into 4 fractions by silica column chromatography, through sequential elution with Hexane (3 ml), Hexane: Dichloromethane (9:1) (1.5 ml), Dichloromethane (5.5 ml) and Ethylacetate:Hexane (20:80) (4 columns) to generate: *n* -alkanes, aromatics, ketone and polar fractions.

The *n*-alkane fraction was analysed by different sets of gas chromatography (GC) configurations for compound quantification and identification. A Thermo Scientific Trace 1310 gas chromatograph was fitted with flame ionization detector (GC-FID) and a split-splitless injector. Compressed air is set as the air flow, helium (He) is set as the carrier flow, nitrogen (N) as a make-up flow and hydrogen (H) helps with ignition. The oven temperature was set at 70 °C for 2 min, then increased to 170 °C at 12 °C min^{-1}, then increased to 310 °C at 6.0 °C min^{-1}, then held at 310 °C for 35 min. *N*-alkanes were separated using a 60 m x 0.25 mm i.d., Restek RXi-5ms column. (0.25 µm 5% diphenyl-95% dimethyl polysiloxane coating). Compound identification was confirmed using a Thermo Scientific Trace 1310 gas chromatography mass spectrometer (GC-MS), equipped with a programmable temperature vaporizer (PTV) injector. He was used as a carrier flow. The oven temperature

Deleted: in

Deleted: g

program was set at 60 °C during 2 min and then raised at 12 °C min^{-1} until reaching 150 °C and then raised again to 310 °C at 6 °C min^{-1} and held for 25 min. Compounds were quantified with reference to internal standards (5α-cholestane) and normalised to the original extracted dry weight of sediment, and to sedimentation rate changes by calculating the mass accumulation rate (MAR). The ratio of higher land-plant derived long-chain *n*-alkanes against aquatic sourced short-chain *n*-alkanes (TAR) (Eq. (1); Cranwell, 1973) and the carbon preference index (CPI) (Eq. (2); Bray and Evans, 1961) were calculated using GC-FID peak areas of the respective compounds:

$$\mathrm{TAR} = \frac{[\mathrm{C27}]+[\mathrm{C29}]+[\mathrm{C31}]}{[\mathrm{C15}]+[\mathrm{C17}]+[\mathrm{C19}]} \qquad (1)$$

$$\mathrm{CPI} = \frac{\frac{[\mathrm{C25{-}33}(\mathrm{odd})]}{[\mathrm{C24{-}32}(\mathrm{even})]}+\frac{[\mathrm{C25{-}33}(\mathrm{odd})]}{[\mathrm{C26{-}34}(\mathrm{even})]}}{2} \qquad (2)$$

Deleted: ¶
High TAR values can be indicative of relative increases in terrigenous organic matter transported to the ocean and/or to relative decreases in aquatic microorganism production. The opposite could explain low TAR values. To disentangle the old organic matter contamination from the fresh signal, we include the CPI index. High CPI values indicate a fresher or relatively newly produced organic matter transported to the ocean. CPI close to 1 indicate mature or old organic matter sources, such as coal or oil deposits, eroded to the ocean.

Terrigenous and aquatic organic matter sources increase during the early Pleistocene in comparison with the late Pliocene. High TAR values can be indicative of relative increases in terrigenous organic matter transported to the ocean and/or to relative decreases in aquatic microorganism production. The opposite could explain low TAR values. To disentangle the old organic matter contamination from the fresh signal, we include the CPI index (Bray and Evans, 1961). High CPI values indicate a fresher or relatively newly produced organic matter transported to the ocean. CPI close to 1 indicate mature or old organic matter sources, such as coal or oil deposits, eroded to the ocean. This distinction may be important in the GOA, where the onshore bedrock includes units with high contents of terrigenous organic matter (e.g. the Yakutat Terrain, Childress, 2016; Walinsky *et al*., 2009).

Alkenones (ketone fractions) were quantified by a GC coupled with chemical ionisation mass spectrometry (GC-CIMS), adapted from the method of (Rosell-Melé *et al*., 1995). Analyses were performed using a Trace Ultra gas chromatograph directly coupled to a Thermo DSQ single quadrupole mass spectrometer, fitted with a programmed temperature vaporising (PTV) injector. 1.2 ml of sample is injected. Alkenones were separated using a 30 m x 0.25 mm i.d., Restek RXi-5ms column (0.25 µm 5% diphenyl-95% dimethyl polysiloxane coating). Helium was employed as the carrier gas (2 ml min^{-1}). The injector was held at 120 °C and splitless mode (1.2 min) during injection, and then immediately temperature programmed from 120 °C to 310 °C at 10 °C s^{-1}, then held for 0.6 min. The oven was programmed to hold at 175 °C for 1.7 min, then increased to 310 °C at 11 min^{-1}, and held at from 310 °C for 12 min. The mass spectrometer was operated in positive chemical ionisation mode (PICI), using high-purity anhydrous ammonia (N6.0, BOC) introduced to the ion source through the CI gas inlet. Selected ion monitoring was performed, targeting the 8 ions corresponding to the $[\mathrm{M + NH4}]^+$ adducts of the target C_{37} and C_{38} alkenones and the internal standard (2-nonadecanone), each with a selected ion monitoring (SIM) width of 1 m z^{-1} and a dwell time of 30 min. The target m z^{-1} were: 300 (2-nonadecanone), 544 ($C_{37:4}$), 546 ($C_{37:3}$), 548 ($C_{37:2}$), as detailed by (Rosell-Melé *et al*., 1995). The alkenone U^{K}_{37}' index has been converted into SST according to the core-top to annual mean SST correlation constructed with samples spanning 60° S to 60° N (including from the Pacific Ocean), which accuracy is constrained by an standard error of ±1.5 °C (Eq. (3); Müller *et al*., 1998). The more recently developed BAYSPLINE SST calibration (Tierney and Tingley, 2018) provides similar SST estimates in the northern latitudes to previous calibrations. The seasonality in the

Deleted: novel

Deleted: than

alkenone production has been evidenced in the North Pacific (Tierney and Tingley, 2018). The SST calibration of Prahl *et al*. (1988) (Eq. (4)), which includes the $C_{37:4}$ alkenone, is also displayed here for comparison, as some concerns have arisen with the use of the U^{K}_{37}' index in samples with high $C_{37:4}$ in the Nordic Seas (Bendle *et al*., 2005). The standard error of Prahl *et al*. (1988) (Eq. (4)) is ±1.0 °C. We identify samples with high $C_{37:4}$ by presenting the percentage of $C_{37:4}$ relative to the other C_{37} alkenones, %$C_{37:4}$ (Bendle and Rosell-Melé, 2004) (Eq. (5)). The %$C_{37:4}$ represents fresher and cooler surface water characteristics (Bendle *et al*., 2005). In the Nordic Seas this has been linked to subpolar and polar water masses (Bendle *et al*., 2005), whereas elsewhere in the North Atlantic it has been linked to freshwater inputs (e.g. during Heinrich events, Martrat *et al*., 2007). In the subarctic Pacific, the %$C_{37:4}$ proxy has been less well studied (McClymont *et al*., 2008), but high %$C_{37:4}$ is also proposed to reflect cooler and fresher water masses (Harada *et al*., 2006).

$$\mathrm{U}^{\mathrm{K}}_{37}{}' = \frac{[C_{37:2}]}{[C_{37:2}]+[C_{37:3}]} = 0.033\mathrm{SST} - 0.044 \qquad (3)$$

$$\mathrm{U}^{\mathrm{K}}_{37} = \frac{[C_{37:2}]-[C_{37:4}]}{[C_{37:2}]+[C_{37:3}]+[C_{37:4}]} = 0.040\mathrm{SST} - 0.104 \qquad (4)$$

$$\%\mathrm{C}_{37:4} = \frac{[C_{37:4}]}{[C_{37:2}]+[C_{37:3}]+[C_{37:4}]}*100 \qquad (5)$$

3.3 IRD

IRD were quantified by weighing the coarse sand fraction (250 μm^{-2} mm) following the method of Krissek (1995). Coarse sand was separated from 10 cm^3 samples by wet sieving after air drying and rinsing with distilled water to remove salts. Each sand sample was examined with a binocular microscope to estimate the volume of terrigenous ice-rafted sediment (in volume percent) in order to exclude biogenic components and burrow fills of manganese and pyrite, which do not have an ice-rafted origin. The mass accumulation rate of IRD (in grams per cm^2 kyr^{-1}) was calculated as in Eq. (6):

$$\mathrm{IRD\ MAR} = \mathrm{CS\%} * \mathrm{IRD\%} * \mathrm{DBD} * \mathrm{LSR} \qquad (6)$$

where CS% is the coarse sand abundance (multiplied as a decimal), IRD% is the IRD abundance in the coarse-sand fraction (as a volume ratio), DBD is the dry bulk density of the whole sediment sample (in grams per cm^3) determined from discrete shipboard measurements and LSR is the interval average linear sedimentation rates (in cm kyr^{-1}).

Closed-form Fourier analysis was used to describe the shape of quartz grains in the IRD fraction imaged on a Quanta FEI 200 Scanning Electron Microscope (in the high vacuum mode at 20 kV) following methods that have been used to describe sedimentary particles for more than 40 years (Ehrlich and Weinberg, 1970; Ehrlich *et al*., 1980; Dowdeswell, 1982; Livsey *et al.,* 2013). Two-dimensional SEM images (from 200 to 500 X magnification) were input into ImageJ to produce a line trace of the boundary for each grain. The output was inspected to verify that the trace was representative of the grain. 120 xy coordinate points were output from the boundary to represent the grain and these were input into the software program PAST (Hammer *et al.,* 2001). Harmonic amplitudes 1-20 were calculated, lower orders (1-10) represent grain shape, a function of provenance and higher order harmonics (11-20) represent grain roundness (Dowdeswell, 1986; Haines and Mazzullo, 1988; Livsey *et al*., 2013). An average dimensionless roughness coefficient (Rca-b) was calculated for each sample using the

Formatted: Font: Italic

Formatted: Font: Italic

Formatted: Subscript

Formatted: Subscript

Deleted: ¶

Deleted: is

harmonics 16-20 for each grain in the population. Higher Rc16-20 values indicate increasing roughness and lower coefficients indicate smoother grains (Dowdeswell, 1982; Livsey *et al.,* 2013). The roughness coefficient is calculated as in Eq. (7):

$$\mathrm{Rc}_{\mathrm{a-b}} = \sqrt{0.5}\,\sum Rn^2 \qquad (7)$$

Where Rn is the nth harmonic coefficient and a-b is the harmonic range used, in our case 16-20 (Ehrlich and Weinberg, 1970). This value represents the average roundness for the grains in each sample, numbering at least 25.

3.4 Pollen Analysis

Palynological treatments were performed on 13 samples according to the procedure routinely used at GEOTOP (de Vernal *et al.,* 1996). Before sieving and chemical treatments, one *Lycopodium clavatum* spore tablet was added in each sample to estimate palynomorph concentrations (Matthews, 1969; Mertens *et al*., 2009). Wet sample volumes were measured by water displacement and weighed after being dried. The fraction between 10 and 120 µm was treated chemically to dissolve carbonate and silicate particles with repeated cold HCl (10 %) and HF (48 %). A small drop of the final residue was mounted on a microscope slide with glycerine jelly. Counting and identification of pollen grains and spores were carried out with a LEICA DM 5000B microscope.

Deleted: Before sieving and chemical treatments, one *Lycopodium clavatum* spore tablet was added in each sample to estimate palynomorph concentrations (Matthews, 1969; Mertens *et al*., 2009).

4 Results and Discussion

4.1 Early and mid-Pliocene (4 to 3 Ma): early Cordilleran Ice Sheet and first glaciation attempts

Early to late-Pliocene (4 to 2.76 Ma) SSTs at Site U1417 are highly variable (max and min SST difference of 10 °C) with an average value of 8.2 °C (Fig. 2; Table 1). We compare our palaeo-SST with the modern SST (here "modern" refers to the averaged decadal statistical mean SST of 6.5 °C (standard deviation of 3.4 °C) during the 1955 to 2012 time period, NOAA WOD13; Boyer *et al*., 2013) at the location of Site U1417 to observe changes in the behaviour of the Alaskan Current. Early to late-Pliocene average SSTs at Site U1417 were approximately 1.7 °C warmer than modern. The Pliocene and Pleistocene SSTs at the GOA have a similar SST range to modern (e.g. NOAA WOD13; Boyer *et al.,* 2013; Fig. 2). The MPWP (3.2 to 3.0 Ma) contains the highest SST peak of the Pliocene, SST=12.4 °C, 5.9 °C warmer than modern SST in the GOA. The average MPWP SST of 8.9 °C is around 2.4 °C warmer than modern. Similar to the MPWP, the MG1-Gi1 warm period (3.6 to 3.4 Ma) contains the second highest peak in SST during the Pliocene, SST=11.7 °C, 5.2 °C warmer SST than modern GOA. Other SST peaks during the MG1-Gi1 are 2-3 °C warmer than modern. The average SST during the MG1-Gi1 period is 9.5 °C, around 3 °C warmer than modern. $C_{37:4}$ concentrations during the Pliocene remain below the threshold of subpolar/subarctic water masses identified in the Nordic Seas (Bendle and Rosell-Melé, 2004) and are consistent with a warm surface ocean and/or minimal meltwater inputs to the GOA. The wide range of "warmer than modern" SSTs occurring during the MPWP together with higher than modern atmospheric CO_2 levels and similar continental configuration, further supports the proposal to use this time period as an analogue for future climate predictions (Hansen, 2006). The MG1-Gi1period

Deleted: which is

Deleted: (here "modern" refers to the averaged decadal statistical mean SST of 6.5 °C during the 1955 to 2012 time period, NOAA WOD13; Boyer *et al*., 2013)

Deleted: period

Deleted: warm period

represents the opportunity for studies to focus on a prolonged period of sustained warm SST but with similar SST peaks than the MPWP.

During the early to mid-Pliocene, IRD is absent and sedimentation rates are the lowest of the 4-1.7 Ma record. Small glaciers in Alaska since or before 4 Ma have been indicated from neodymium and lead isotope records from the Bering Sea (Horikawa *et al*., 2015). However, our data show that during the early and mid-Pliocene, the Cordilleran Ice Sheet was not yet extensive enough to erode or transport large volumes of sediment and runoff to the GOA. In contrast, IRD at ODP Site 887 (located 200 km southwest of U1417) suggests glacial influence in the GOA since 5.5 Ma (Reece *et al*., 2011). Early Pliocene and even Miocene evidence of tidewater glaciation ($\delta^{18}O$, IRD) has been found at other locations in the North Atlantic (Mudelsee and Raymo, 2005; Bachem *et al*., 2016). Reece *et al.* (2011) attributed the initiation of glaciation in the GOA to the uplift of the Yakutat formation. However, IRD mass accumulation rates at ODP 887 prior to 2.6 Ma are very small, being close to 0 and < 0.2 g cm^{-2} Ky^{-1} (Krissek, 1995). The low sedimentation rate, high TAR, low $\%C_{37:4}$ and absence of IRD during this period at Site U1417 suggest that although the GOA experienced intervals of relatively cool SSTs (Fig. 2a), limited mountain glaciation but not full-scale continental glaciation resulting in tidewater glaciers marked the early and mid-Pliocene presented here.

There are two intervals of significant cooling recorded during the Pliocene at Site U1417: the MIS M2 (3.3 Ma) and KM2 (3.2 Ma) (Fig. 2a). Neither of these cold intervals record IRD delivery to Site U1417. Both intervals are punctuated by core breaks, suggesting a change in the sediment lithology which made core recovery difficult (Fig. S1). The M2 has been proposed as a significant Pliocene glaciation, though smaller than early Pleistocene glaciations, possibly due to the prevalent high atmospheric CO_2 levels (De Schepper *et al*., 2013) (Fig. 3a). However, if this event, and the climatic conditions we record in the GOA, triggered the appearance of glaciation in Alaska at all (De Schepper *et al*., 2013), our data suggests the glaciation was not intense enough to support an ice sheet with a tidewater margin that delivered icebergs to Site U1417. Our record provides evidence for relatively cold SST conditions during M2, as cold as conditions during major glacial cycles of the Pleistocene, but with no evidence for the development of a major Cordilleran Ice Sheet.

Between 4 and 3 Ma ago, we observe maximum TAR values (up to 16; Fig. 2), pointing to a higher export of terrigenous (i.e. land-plant leaf waxes) relative to aquatic organic matter to the GOA. We assume that the warm and wet climate of the early Pliocene during high atmospheric CO_2 levels potentially sustained a highly vegetated landscape in Alaska and west Canada which delivered high amounts of plant wax lipids and pollen grains into the GOA. The absence of IRD and higher pollen counts may refer to an airborne transport of the leaf wax lipids rather than an export via icebergs. The colder SST during the Pliocene could have promoted a deeper AL and dust driven transport of terrigenous organic matter may have developed. Strong winds could have transported plant waxes to Site U1417 during the Pliocene, as is also observed in the North Atlantic during the NHG (Naafs *et al*., 2012). Müller *et al*. (2018) also proposed an export of long-chain *n*-alkanes to the GOA via dust storms. We suggest that, in addition to wind transport, also coastal river discharge of terrigenous organic matter may have contributed to higher TAR values recorded at Site U1417.

Deleted: organic matter

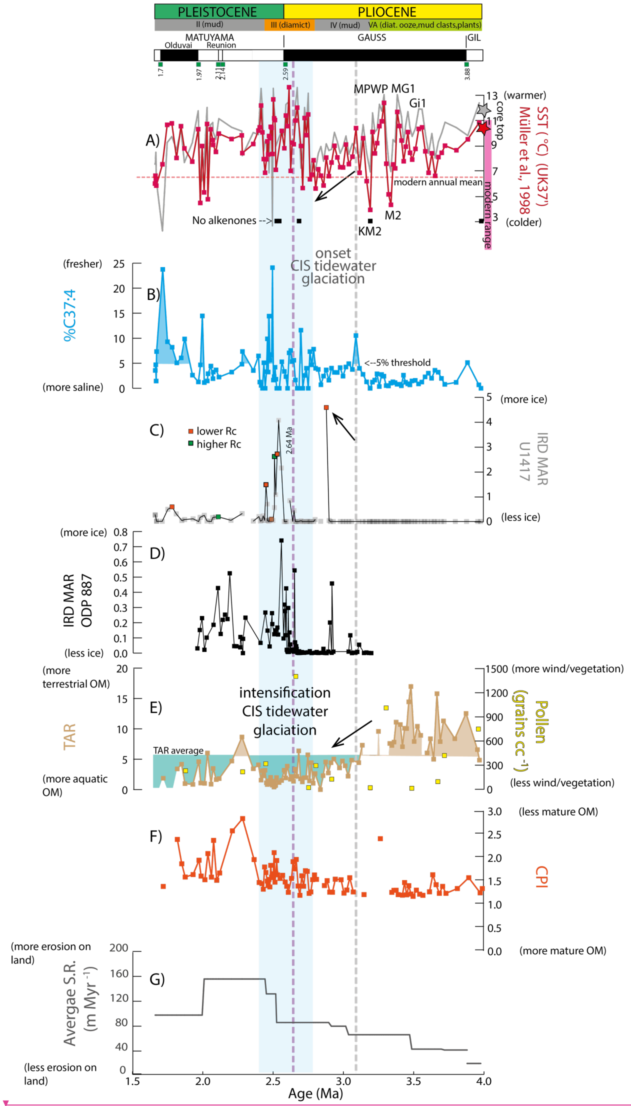

Deleted:

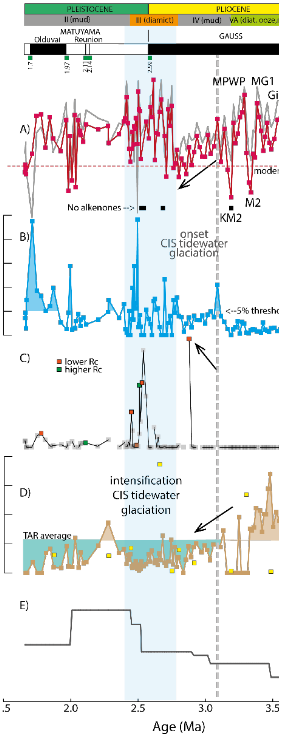

Formatted: Centered

Figure 2: Site U1417 across the Pliocene-Pleistocene transition. a) red line: SST from U^{K}_{37}’ index according to Müller *et al*. (1998) calibration; grey line: SST from U^{K}_{37} index according to Prahl *et al.* (1988) calibration. Black squares are samples where alkenones were not detected. Dashed red line: Modern averaged decades (1955-2012) annual statistical mean SST=6.4 °C at 0 m water depth (NOAA WOD13, Boyer *et al.,* 2013) at Site U1417, similar to the modern annual average SST=7 °C at GAK1 station during the 1970-2018 time intervals for the 0-100 m water column depth (Weingartner *et al*. 2016) in the Gulf of Alaska; Red star on y-axis: value of our youngest sample analysed at Site U1417 (U1417D 1H-1W 44-48; 0.016 Ma; SST=10.6 °C with Müller *et al*. (1998) calibration; SST=11.8 °C with Prahl *et al.,* 1988 calibration); Pink rectangle on y axis: modern averaged decades (1955-2012) statistical mean SST during winter and summer at Site U1417 and 0 m water depth (NOAA WOD13, Boyer *et al.,* 2013) SST=0-11,3 °C; b) abundance of the cold and freshwater alkenone $C_{37:4}$ (%). Horizontal line shows the threshold of Bendle *et al*. (2005) above which subarctic/subpolar water masses were determined for the Nordic Seas; c) IRD MAR (g cm^{-2} ka^{-1}). Orange and green squares reflect lower and higher average roughness coefficient (Rc) of the IRD quartz grains, respectively; d) IRD MAR (g cm^{-2} ka^{-1}) at ODP 887 (Prueher and Rea, 2001); e) terrestrial/aquatic *n*-alkane index (TAR), horizontal line shows the average TAR value, yellow squares represent pollen grains concentrations in grains cc^{-1} and f) CPI and g) average sedimentation rates (see Fig. S3b) in m Myr^{-1} at Site U1417. Upper panel: Pliocene-Pleistocene boundary, magnetostratigraphy events and interpretations (see Fig. S2 and S3) and Lithostratigraphic units of Site U1417 with simplified lithology (orange colouring represents ice rafted diamict interbedded with mud, brown colouring represents marine mud and green colouring represents diatom ooze interbedded with debris flow deposits containing mud clasts and plant fragments) (Jaeger *et al*., 2014). Grey vertical line represents the onset of the Cordilleran Ice Sheet (CIS) glaciation (or oNHG) climate transition at 3 Ma, blue shading represents the 2.5-2.0 Ma climate transition with the intensification of the Cordilleran Ice Sheet (CIS) tidewater glaciation (or iNHG) as in Table 1. Purple vertical line represents the onset of the Cordilleran Ice Sheet at the Lower Klondike Valley, Yukon interior (Hidy *et al*., 2013; Fig. 1). Missing data points are either a result of samples analysed for SSTs at the early stages of the project which were not subsequently analysed for n-alkane distributions, and the result of samples where chromatograms reflected poorly resolved *n*-alkane peaks.

We further note that rivers and ocean currents could have transported bedrock material from the Yakutat Terrain (Childress, 2016) to Site U1417, 700 km offshore from the Alaskan coast. This would imprint the sediments delivered to the ocean with an ancient signal of terrigenous organic matter, rather than reflecting erosion of contemporary ‘fresh’ organic matter from vegetation and soils. The CPI is often used to estimate the maturity of the organic matter and determine its source. Previous studies suggest that elevated TAR values and CPI values close to 1 reflect coal particles found in sediments in the GOA (Rea *et al*., 1995; Gulick *et al*., 2015). However, the coal-bearing Kulthieth rocks (McCalpin *et al*., 2011), have a TAR signature of a maximum value of 2 (Childress, 2016). Since Site U1417 TAR (up to 16) and CPI values (> 1) do not overlap with TAR (up to 2) and CPI (< 1) values found onshore (Childress, 2016), the TAR and CPI values at Site U1417 thus suggest a mix of sources of organic matter during this time dominated by contemporaneous vegetation, although we cannot exclude the possibility of some coal erosion.

4.2 The late Pliocene onset of the Cordilleran Ice Sheet glaciation (3 to 2.8 Ma)

The interval from 3 to 2.8 Ma is characterised by a shift of climate conditions from those observed during the early and mid-Pliocene (Fig. 2) to more glacial conditions. At 3 Ma, average SSTs at Site U1417 remain relatively warm (around 8 °C), yet, there is the first cooling evidence at Site U1417 deduced from $C_{37:4}$ crossing the threshold of 5 % (Bendle *et al.*; 2005). %$C_{37:4}$ increases can be related to colder sea surface conditions, but due to Site U1417’s location and climatic context, we suggest that increases in %$C_{37:4}$ relate to meltwater discharge from the expanding ice-sheet. From 3.1 to 2.8 Ma, SST decreases gradually from 8 to 5.5 °C (Fig. 2a) recording again colder SSTs than the modern GOA. We attribute this 0.3 Ma progressive cooling to the oNHG in response to the overall decrease in the atmospheric CO_2 (Seki *et al.,* 2010; Martínez-Botí *et al*., 2015). From 3 Ma, TAR values decrease to below the average of the entire TAR record, indicating that transport of leaf-wax lipids to Site U1417 increased in comparison with the Pliocene, which may be related to an increase in erosion on land due to the

Deleted: e

Deleted: from

Deleted: V

Deleted: grey

Formatted: Font: Italic

Deleted: we exclude a bedrock source to be driving the TAR variations at Site U1417.

Deleted: might

Deleted: from

Deleted: land

Deleted: and

Deleted: of

Deleted: erosion

Deleted: evidence for a

Deleted: at

Deleted: slightly decreased

Deleted: reduction in vegetational growth on

Deleted:

advancing ice-sheet. The coincident increase in average sedimentation rates (from 65 to 79 m Myr^{-1}) indicates a more efficient erosive agent onshore than before 3 Ma and/or a change in the source of terrestrial matter. However, CPI values at Site U1417 (Fig. 2e) remain similar to early and mid-Pliocene values, which suggests a similar source of the terrigenous organic matter. The most reasonable explanation is that the land was becoming increasingly ice covered, so that the erosion of vegetation and terrigenous organic matter eroded and transported to the ocean increased.

The peak in %C$_{37:4}$ at 3 Ma is followed by lower %C$_{37:4}$ values (close to 5 %) and the first significant pulse of IRD identified by a single sample with the highest IRD MAR. This IRD MAR peak (4.5 g cm^{-2} ka^{-1}) and an increase in sedimentation rates (from 79 to 85 m Myr^{-1}) at 2.9 Ma constitute the first evidence that tidewater glaciers were present in southwest Alaska delivering icebergs to Site U1417. IRD quartz grains do not appear crushed or abraded by glacial activity indicating small tidewater valley glaciers producing icebergs which could contain grains that were introduced by rockfall or fluvial sediment. The abrupt peak in IRD delivery to U1417 at 2.9 Ma could be due to ice growth on land and cold enough SSTs to permit distal iceberg-drift and release of debris to Site U1417. The increase in sedimentation rate has been suggested to mark the maximum Cordilleran Ice Sheet extension during the Pliocene (Gulick *et al*., 2015). Following this first peak, IRD MAR decreases to values between 0 and 1 g cm^{-2} ka^{-1} until 2.6 Ma. This abrupt decrease in IRD indicated lower iceberg delivery to Site U1417. A synchronous increase of C$_{37:4}$ above 5 % suggests the melting of tidewater glaciers was responsible for the decrease in iceberg delivery despite the cold SST. Atmospheric CO$_2$ concentration peaks during this time (Fig. 3a) may have contributed to a reduced ice sheet due to radiative forcing.

4.3 The intensification of the Cordilleran Ice Sheet glaciation (2.7-2.4 Ma) and its evolution during the early Pleistocene (2.4-1.7 Ma)

At Site U1417, the iNHG during the Plio-Pleistocene transition (PPT) is characterised by a rise in SST, followed by highly variable values (between 5.6 to 13.6 °C) with an average of 9.7 °C, 3.2 °C warmer than modern. The iNHG is defined here as the period containing sustained signs of glaciation (i.e. Maslin *et al.*,1996; Bartoli *et al*., 2005), which at Site U1417 are confirmed by glacial meltwater and IRD delivery. The relatively high %C$_{37:4}$ (up to 24 %) in the early Pleistocene correlates well with the period of high IRD delivery (up to 4 g cm^{-2} Ka^{-1}) between 2.7 to 2.4 Ma (Fig. 2b and c). This suggests this period marks an expansion/intensification of the Cordilleran glaciation following a gradual SST cooling during the oNHG. The timing of the increase in IRD at Site U1417 coincides with the increase in IRD at Site 887 (St John and Krissek, 1999) and the maximum extent of the CIS as recorded onshore in the eastern Cordillera by the extensive Klondike gravels at 2.64 Ma (+0.20/-0.18 Ma) (Hidy *et al.*, 2013). The lithology at Site U1417 includes diamict layers that alternate with bioturbated mud from 2.7 Ma, indicating that the Cordilleran Ice Sheet remained very variable after the oNHG and maintained glacial tidewater margins discharging icebergs into the sea. Yet the intensification of the Alaskan tidewater glaciation occurred with a GOA that was overall either warmer than, or at least as warm as the mid to late Pliocene (considering Müller *et al*. 1998 SST calibration error).

Deleted: Alternatively

Deleted: , if

Deleted: , the growth of vegetation and the abundance of terrigenous organic matter that could be eroded and transported to the ocean would have declined, even if erosion rates as a whole increased. …

Deleted: the

Deleted:

Deleted: of ±1.5 °C

The overall increase in %C$_{37:4}$ in the GOA during the early Pleistocene coincides with an SST warming (ca. 1 °C relative to the Pliocene; Fig. 2a and b), suggesting a stronger link between C$_{37:4}$ and meltwater fluxes rather than an expansion of subarctic water masses. Additionally, maxima and minima in %C$_{37:4}$ during the iNHG are unrelated to elevated or lowered SSTs, respectively. There is no information available about the origin of C$_{37:4}$ in the North Pacific to explain the high %C$_{37:4}$ values recorded at Site U1417, nor their association with intermediate SSTs rather than minima/maxima. It has been suggested that stratification of the water column due to glacier discharge in the North Pacific could result in warmer sea surface in comparison to deeper water masses due to an increase in surface absorption of solar radiation (Meheust *et al*., 2013). Haug *et al*. (2005) proposed this could lead to an increase in ocean evaporation and orogenic precipitation, ultimately encouraging North American ice sheet growth.

Over the iNHG, low TAR values (< 1) and small variations in IRD MAR (the order of 0.1 to 2.8 g cm^{-2} Ka^{-1}) coincide with intermediate SSTs (7 to 11 °C) and %C$_{37:4}$ between (2-24 %). This could point to an increase in marine productivity export related to an enhanced nutrient delivery to Site U1417 via glacial runoff. The CPI values discard mature sources of organic matter to the GOA at this time interval suggesting a contemporary aquatic organic matter contribution. IRD peaks are typically present during SST minima suggesting the importance of SSTs in the delivery of icebergs to distal sites such as Site U1417. The average Rc of IRD is low (Fig. 2c) even during IRD MAR peaks, indicating minimal glacial crushing during the iNHG. In comparison, samples from 1.6 - 1.5 Ma show a higher Rc and appear to have greater evidence of glacial crushing, suggesting development of a larger ice sheet or scouring and evacuation of sediment from the non-glacial, weathered landscape. This could indicate that the first IRD in icebergs delivered to the GOA during the late Pliocene and early Pleistocene originated from smaller marine terminating valley glaciers which removed sediment and weathered rock from the landscape rather than eroding bedrock and allowed IRD generation.

Deleted: at first

Deleted: The IRD Rc characterization suggests landscape changes that could explain the smaller variations in TAR during the early Pleistocene.¶

The comprehensive data set obtained from Site U1417 sediments (Fig. 2) supports a climate role in the ice-sheet expansion during the early Pleistocene and the iNHG, with an increase in precipitation from a warmer and/or stratified ocean, and cooler periods associated with IRD delivery. An additional explanation for the changing TAR during the early Pleistocene is that tectonic uplift of the Chugach/St Elias area from 2.7 Ma (Enkelmann *et al*., 2015) led to orogenic precipitation and a change in erosional pathways (Enkelmann *et al*., 2015). The glaciation could have altered the main source of terrestrial input to the Surveyor Channel, to higher metamorphic and plutonic sources with lower or null TAR values (Childress, 2016). An increase in CPI variability to concentrations up to 2 and 3 during the early Pleistocene (starting from 2.7 Ma) supports the change of source of organic matter away from the more mature coal bedrock into more immature terrestrial organic matter (plant waxes). However, this comes at a time of increasing IRD, which adds a new source of terrigenous sediment to Site 1417. The shift in CPI values at 2.7 Ma agrees with the shift towards the erosion of sediments sourced from metamorphic and plutonic sources, described in Enkelmann et al. (2015) delivered to Site U1417. Lower pollen counts suggest a less vegetated landscape, which could help explain the overall lower TAR during the early Pleistocene in comparison with the Pliocene.

Deleted: alternative, or

Deleted: ,

Deleted: An increase in CPI variability to 2 and 3 during the early Pleistocene support the change of source of organic matter delivered to Site U1417 away from the more mature coal bedrock.

4.4 The Pliocene and Pleistocene climate across the North Pacific Ocean.

The overall cooling trend during the Neogene, briefly interrupted by the MPWP and intense cooling events such as the M2, is believed to be a dominant pattern in the global climate. This notion is largely based on the global increase in ice volume (e.g. LR04 Benthic δ^{18}O Stack (Lisiecki and Raymo, 2005) and from studies in the North Atlantic SST (i.e. ODP Site 982, Lawrence *et al*., 2009). In contrast, the contribution of the North Pacific into our understanding of the global climate evolution from the Pliocene to the Pleistocene is limited. Our study at Site U1417 adds valuable regional climate information during the evolution of the Cordilleran Ice Sheet. Unlike the LR04 stack, average Pliocene SST values (4.0 to 2.8 Ma) at Site U1417 are 1 °C colder than the average early Pleistocene values (2.7 to 1.7 Ma) (the Pliocene-Pleistocene SST difference of 1°C has an standard deviation of 0.5°C). In the wider North Pacific, a warming trend from the late Pliocene to early Pleistocene has also been observed at ODP Site 882 in the subarctic Pacific (Martínez-García *et al*., 2010), at Site 1010 and potentially at Site 1021 (mid-latitude east Pacific) (Fig. 3). Beyond the North Pacific, warmer SST during the early Pleistocene compared to the Pliocene have also been recorded i.e. DSDP Site 593 in the Tasman Sea (McClymont *et al*., 2016) and Site 1090 (Martínez-García *et al*., 2010) in the South Atlantic. In contrast, long-term cooling trends mark the early Pleistocene for the mid-latitude west Pacific (Site 1208) and tropical east Pacific (Site 846), more consistent with the development of a cooler and/or more glaciated climate (Fig. 3).

Formatted: Font: (Default) Times New Roman, 10 pt

Formatted: Font: (Default) Times New Roman, 10 pt

Formatted: Font: (Default) Times New Roman, 10 pt

The North Pacific warming occurs despite an atmospheric CO_2 drop from 280-450 ppmv to 250-300 ppmv (similar to pre-industrial levels) from 3.2 to 2.8 Ma (Pagani *et al*., 2010; Seki *et al*., 2010) and an associated reduction in global radiative forcing (Foster *et al*., 2017). The early Pleistocene warming signal in the GOA (and the north Pacific more generally) thus implies an important role for local or regional processes. We have discussed above the potential role played by ocean stratification in the North Pacific, and a possible link to the evolving Cordilleran Ice Sheet in the GOA through evaporation/precipitation feedbacks. The synchrony of these changes with observed tectonic uplift (e.g. Enkelmann *et al*. 2015) makes it difficult to disentangle the potential climatic and tectonic mechanisms behind ice sheet expansion.

To understand the evolution of the ocean currents governing the North Pacific at the present core sites (Fig. 1) and to find possible explanations of the observed SST distributions during the Pliocene and Pleistocene climate evolution, the modern climate system is used here as an analogue. Modern monthly mean SSTs at ODP 882 SSTs are colder than Sites U1417 and 1021 all year around. During the late Pliocene and early Pleistocene, ODP 882 SSTs are 3-4 °C warmer than in the east (Fig. 3f and g). Modern seasonal climate analogues cannot be used to explain to Pliocene and Pleistocene subarctic SST distribution. However, on longer timescales, the strength of the AL is currently linked to the wider Pacific Ocean circulation by the Pacific Decadal Oscillation (PDO) over periods of 20-30 years (Furtado *et al*., 2011). The Pliocene-Pleistocene North Pacific SST gradients show similarities with the negative phase of the PDO (-PDO), which is characterized by positive SST anomalies in the central North Pacific surrounded by negative SST anomalies along the North American coast and in the east equatorial

Pacific. The -PDO associated route of winds might have increased the precipitation in the Gulf of Alaska and represent a key factor for the fast building of ice in the Alaskan mountains.

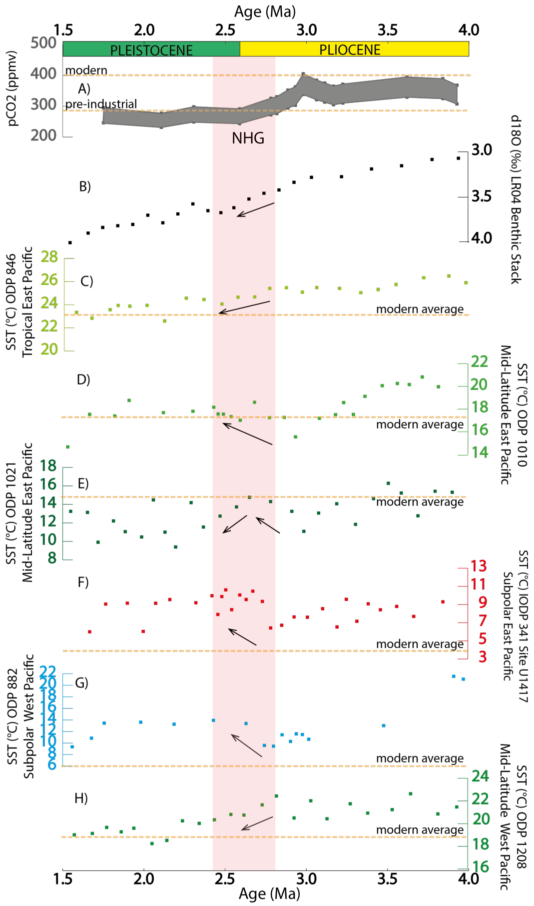

5 **Figure 3**: **Pliocene-Pleistocene SST across the North Pacific.** a) Alkenone pCO$_2$ upper and lower end (ppmv) estimates at Site ODP 999A (Seki *et al.,* 2010); b) δ^{18}O (‰) LR04 Benthic Stack (Lisiecki and Raymo, 2005); Alkenone SST (°C) from c) ODP Site 846 (Herbert *et al*., 2017), d) Site 1010 (Herbert *et al.,* 2018), e) Site 1021 (Herbert *et al.,* 2018), f) IODP 341 Exp. Site U1417 (Sánchez-Montes *et al*., 2019), g) ODP Site 882 (Martínez-García *et al.,* 2010) and h) ODP Site 1208 (Herbert *et al.,* 2018). Orange horizontal lines indicate reference levels

Deleted: Average Pliocene SST values (4.0 to 2.8 Ma) at Site U1417 are 1 °C colder than the average early Pleistocene values (2.7 to 1.7 Ma). A warming trend from the late Pliocene to early Pleistocene observed at Site U1417 has also been observed at ODP Site 882 in the subarctic Pacific (Martínez-García *et al*., 2010), DSDP Site 593 in the Tasman Sea (McClymont *et al*., 2016) and Site 1090 (Martínez-García *et al*., 2010) in the South Atlantic. These warmings contrast with the gradual surface cooling from the Pliocene to present within the North Atlantic (e.g. ODP Site 982, Lawrence *et al*., 2009). The North Pacific warming occurs despite an atmospheric CO$_2$ drop from 280-450 ppmv to 250-300 ppmv (similar to pre-industrial levels) from 3.2 to 2.8 Ma (Pagani *et al*., 2010; Seki *et al*., 2010) and an associated reduction in global radiative forcing (Foster *et al*., 2017). This warming signal in the GOA (and the north Pacific more generally) implies an important role for local or regional processes. We have discussed above the potential role played by ocean stratification in the North Pacific, and a possible link to the evolving Cordilleran Ice Sheet in the GOA through evaporation/precipitation feedbacks. The synchrony of these changes with observed tectonic uplift (e.g. Enkelmann *et al*. 2015) makes it difficult to disentangle the potential climatic and tectonic mechanisms behind ice sheet expansion

Formatted: Font: (Default) Times New Roman

Deleted: By comparing the Site U1417 SST records with others recovered from the North Pacific Ocean (Fig. 3), the following patterns emerge. All records, which range from the equator to the subarctic (Fig. 3), show warm SST during the MG1-Gi1 and the MPWP. All show orbital scale SST oscillations, including cooling during the M2 and KM2 cold events which interrupt late Pliocene warmth (Fig. 3). All records show a cooling interval immediately following the MPWP (~3.0-2.7 Ma). The subsequent warming from 2.7 Ma observed at the subarctic Pacific Sites U1417 and 882 is also identified at Site 1010 and potentially at Site 1021 (mid-latitude east Pacific). In contrast, long-term cooling trends mark the early Pleistocene for the mid-latitude west Pacific (Site 1208) and tropical east Pacific (Site 846). This cooling trend is more consistent with the development of a cooler and/or more glaciated climate as recorded in the benthic δ^{18}O stack (Fig. 3) and in SST data from the Atlantic Ocean (e.g. ODP Site 982, Lawrence *et al*., 2009). The regional scale warming into the early Pleistocene observed in the subarctic Pacific and mid-latitude east Pacific suggests that while local factors such as tectonic uplift could have been involved in the Cordilleran Ice Sheet development and might have influenced the SST in the GOA, the GOA climate signals reflect a wider scale warming in the mid to high latitude Pacific.¶ ... [1]

Formatted: Centered

Deleted:

Deleted: d^{18}O

Formatted: Superscript

of pre-industrial times and/or modern values for each of the records or sites (SSTs from NOAA WOD13, Boyer *et al.*, 2013). Arrows indicate position of M2 and KM2 periods and cooling or warming trends across the Pacific Ocean. The KM2 event is located within the MPWP. The MG1-Gi warming precedes the M2 event. b) to h) climate data are 100 kyr smoothed records, and the x axis have been determined through the calculation of the mean for each interval.

5 Conclusions

The sea surface temperature (SST) evolution from the Pliocene to the early Pleistocene in the subarctic Northeast and east-mid latitude North Pacific is very different from the North Atlantic, with a colder Pliocene than early Pleistocene. The early Pliocene appears to be characterised by a heavily vegetated landscape where there is no obvious noticeable glaciation in the St. Elias mountains. A series of cooling events during the Pliocene (including the M2 event) could have initiated glaciation in Alaska but it was limited to mountain glaciers probably due to high atmospheric CO_2 concentrations and the lower topography in coastal Alaska. The first evidence of glaciation starts at 3 Ma with an increase in glacial meltwater followed by a progressive 2.5 °C SST cooling from 3.1 to 2.8 Ma and the first IRD peak at 2.9 Ma since the late Pliocene. Glacial meltwater, IRD and sedimentation rates increase, identified as the intensification of the Cordilleran glaciation (2.7-2.4 Ma). This occurs with warm SSTs suggesting an efficient warm ocean-land precipitation-Cordilleran Ice Sheet growth interactions.

A permanent warm surface ocean in the west mid-latitude Pacific during the late Pliocene and early Pleistocene compared to modern was potentially a key mechanism for increasing moisture supply to the Gulf of Alaska (GOA) and triggering the growth of the Cordilleran Ice Sheet. A similar to modern negative PDO-like climate could have set a more efficient route for moisture transport from the west subarctic Pacific to the GOA since the MPWP and could have been a key mechanism for glacial growth. Unlike during the Pliocene, the early Pleistocene drop in atmospheric CO_2 concentrations could have been decisive in developing a continuous glaciation of the Cordilleran Ice Sheet during the variable climate of the intensification of the Cordilleran tidewater glaciation. However, the synchronous tectonic uplift of the St Elias mountains could also have been a contributing factor for the Cordilleran Ice Sheet expansion, increasing the potential for precipitation as snow over the ice sheet source regions, despite warm SST in the GOA.

Deleted: To understand the mechanisms that caused warmer SSTs to develop across the North Pacific under lower atmospheric CO_2 levels, the modern climate system is used here as an analogue to infer feasible changes in ocean and atmospheric circulation. During the Pliocene and Pleistocene, warm events are marked by a decrease in the latitudinal and longitudinal SST gradients than during cold periods (Table 3). SST gradients reduce greater on the east than the west Pacific and to a lesser decree between east and west Pacific (Table 3). These patterns aren't consistent with modern winter/summer circulation respectively (Fig. 1), where there is a longitudinal seesaw in SST gradients: during modern winter (Fig. 1b) latitudinal SST gradients increase in the east and decrease in the west Pacific and the opposite occurs during summer (Fig. 1c). Consequently, longitudinal east-west SST gradients increase during winter and the heat budget of the west increases in comparison to the east during summer. This seems to be caused by a great seasonal SST difference at Site 1208 during modern winter, where SST cools up to 10 °C. During the strongest AL during winter, wind and ocean currents efficiently cool the entire North Pacific, especially the west mid-latitudes. During the summer weakening of the AL and weaker atmospheric and ocean circulation, leads to warming of the North Pacific at all latitudes. During the Pliocene and Pleistocene, the latitudinal SST gradients are similar to, or increased in comparison to modern and longitudinal SST gradients are comparable or reduced ... [2]

Formatted: Font color: Red

Formatted: Space Before: 0 pt, After: 0 pt, Line spacing: 1.5 lines

Deleted: late

Deleted: weak, negative Pacific Decadal Oscillation "PDO-like" circulation

Deleted: ,

Deleted: and the inefficient supply of moisture to the high latitudes. …The ... [3]

Deleted: The

Deleted: overall increase in latitudinal SST gradients and

Deleted: stable

Deleted: for

Deleted: A reversal of the east-west SST gradient relative

Deleted: today and similar to

Deleted: been

Deleted: mechanism

Deleted: of deliver

Deleted: ing

Deleted: moisture

Deleted: from the west subarctic Pacific to the subarctic

Deleted: During warm periods, the enhanced negative PDO-like climate with the associated changes in atmospheric and ocean ... [4]

Deleted: T

Deleted: Moisture supply to the GOA by an enhanced -PDO like climate is a key mechanism for glacial growth during the early ... [5]

Data availability

The data presented in this manuscript has been submitted to Pangaea.de and it is under review. After the publication of this manuscript, the data would be accessible through this link https://doi.org/10.1594/PANGAEA.899064 and could be cited as Sánchez-Montes *et al*. (2019). The SST data in this publication will also be published in the PlioVAR database.

Author contribution

New data sets presented in this manuscript derive from the PhD project of MLSM supervised by ELM and JML. JM was closely engaged from early stages of this project including aspects of method development. EAC generated the IRD data, and CZ generated pollen data. All authors have contributed to data interpretations. MLSM prepared the manuscript with contributions from all co-authors.

Acknowledgements

We would like to acknowledge the International Ocean Discovery Program U.S. Implementing Organization (IODP-USIO) and the captain and crew of the D/V *Joides Resolution*. This work was supported by funding from Van Mildert College and the Durham Doctorate Scholarship (MLSM), the Philip Leverhulme Prize (ELM), and a NERC-IODP grant (NE/L002426/1) to ELM. JM received funding through the German Research Foundation (MU3670/1-2), an ECORD grant and the Helmholtz Association (VH-NG-1101). EAC received funding from U.S. National Science Foundation award OCE-1434945 and a post-expedition award from the U.S. Science Support Program of the IODP. We thank valuable comments from Professor Joseph S. Stoner on our new age model proposed here. We thank Martin West, Amanda Hayton and Kathryn Melvin for assistance with the GCMS analyses, and Mathew Sandefur and Hugh Harper for assistance with the IRD analyses. This work is a contribution to the PlioVAR working group synthesis of Pliocene marine data (http://pastglobalchanges.org/). We thank Alberto Reyes (CP editor) and CP reviewers Anders Carlson and a second anonymous reviewer for valuable discussions and comments that helped in shaping this manuscript.

References

Andreev, A. A., Trasov, P. E., Weenrich, V., Raschke, E., Herzschuh, N. R., Bringham-Grette, J. and Melles, M., Late Pliocene and Early Pleistocene vegetation history of northeastern Russian Arctic inferred from the Lake El'gygytgyn pollen record, Clim. Past, 10, 1017-1039, 2014.

Bachem, P.E., Risebrobakken, B. & McClymont, E.L. Sea surface temperature variability in the Norwegian Sea during the late Pliocene linked to subpolar gyre strength and radiative forcing. Earth and Planetary Science Letters, 446:113- 122, 2016.

Bartoli, Gretta; Sarnthein, Michael; Weinelt, Mara; Erlenkeuser, Helmut; Garbe- Schönberg, Carl-Dieter; Lea, David W, Final closure of Panama and the onset of northern hemisphere glaciation. Earth and Planetary Science Letters, 237, 33-44, doi:10.1016/j.epsl.2005.06.020, 2005.

Bendle, J. A.; Rosell-Melé, A., Ziveri, P., Variability of unusual distributions of alkenones in the surface waters of the Nordic seas, Paleoceanography, 20(2), PA2001, doi:10.1029/2004PA001025, 2005.

Bendle, J. A. and Rosell-Melé, A., Distributions of UK37 and UK37' in the surface waters and sediments of the Nordic Seas: implications for paleoceanography. Geochemistry, Geophysics, Geosystems 5, Q11013-Q11013, doi:10.1029/2004GC000741, 2004.

Boyer, T.P., Antonov, J. I., Baranova, O. K, C. Coleman, C., García, H. E., Grodsky, A., Johnson, D. R., Locarnini, R. A. Mishonov, A. V., O'Brien, T.D., Paver, C.R., Reagan, J.R., Seidov, D., Smolyar, I. V. and Zweng, M. M., World Ocean Database, NOAA Atlas NESDIS 72, S. Levitus, Ed., A. Mishonov, Technical Ed.; Silver Spring, MD, 209 pp., http://doi.org/10.7289/V5NZ85M , 2013.

Bray, R. R. and Evans, E. D., Distribution of n-paraffins as a clue to recognition of source beds, Geochimica et Cosmochimica Acta, 22, 2-15, 1961.

Bringham-Grette, J., Melles, M., Minyuk, P., Andreev, A., Tarasov, P., Deconto, R., Koenig, S., Nowaczyk, N., Wennrich, V, Rosén, P., Haltia, E., Cook, t., Gebhardt, C., Meyer-Jacob, C., Snyder, J., Herzschuh, U., Pliocene warmth, polar amplification, and stepped pleistocene cooling recorded in NE Arctic Russia, Science, 340(6139), 1421-1427, https://doi.org/10.1126/science.1233137, 2013.

Childress, L. B., The Active Margin Carbon Cycle: Influences of Climate and Tectonics in Variable Spatial and Temporal Records, PhD thesis Northwestern University, Evanson, Illinois, 2016.

Cranwell, P. A, Chain-length distribution of n-alkanes from lake sediments in relation to post-glacial environmental change, Freshwater Biol. 3:259-265, 1973.

De Shepper, S., Groeneveld, J., Naafs, B. D., Van Renterghem, C., Hennissen, J., Head, M. J., Louwye, S. and Fabian, K., Northern Hemisphere Glaciation during the Globally Warm Ealy Late Pliocene, PLOS ONE, Vol. 8, Issue 12, 1-15, 2013.

de Vernal, A., Henry, M., Bilodeau, G., Micropaleontological preparation techniques and analyses. Les Cahiers du Geotop 3, 16–27, 1996.

Dolan, A. M., Haywood, A. M., Hill, D. J., Dowsett, H. J., Hunter, S. J., Lunt, D. J. and Pickering, S. J., Palaeogeography, Palaeoclimatology, Palaeoecology 309, 98-110, 2011.

Dolan, A. M., Haywood, A. M., Hunter, S. J., Tindall, J. C., Dowsett, H. J., Hill, D. J. and Pickering, S. J., Modelling the enigmatic Late Pliocene Glacial Event, Marine Isotope Stage M2, Global and Planetary Change 128, 47-60, 2015.

Dowdeswell, J.A., Scanning electron micrographs of quartz sand grains from cold environments examined using fourier shape analysis, Journal of Sedimentary Petrology 52, 1315-1323, 1982.

Dowdeswell, J.A., The distribution and character of sediments in a tidewater glacier, southern Baffin Island, N.W.T., Canada, Arctic and Alpine Research 18, 45-56, 1986.

Ehrlich, R. and Weinberg, B., An exact method for characterization of grain shape, Journal of Sedimentary Petrology 40, 205-212, 1970.

Ehrlich, R., Brown, P.J., Yarus, J.M. and Przygocki, R.S., The origin of shape frequency distributions and the relationship between size and shape, Journal of Sedimentary Petrology 50, 475-483, 1980.

Enkelmann, Peter O. Koons, Terry L. Pavlis, Bernard Hallet, Adam Barker, Julie Elliott, John I. Garver, Sean P. S. Gulick, Rachel M. Headley, Gary L. Pavlis, Kenneth D. Ridgway, Natalia Ruppert, Harm J. A. Van Avendonk. Cooperation among tectonic and surface processes in the St. Elias Range, Earth's highest coastal mountains. Geophysical Research Letters, 42 (14): 5838 DOI: 10.1002/2015GL064727, 2015.

Fedorov, A. V., Lawrence, K. T., Liu, Z., Dekens, P. S., Ravelo, A. C., and Brierley, C. M.: Patterns and mechanisms of early Pliocene warmth, Nature, 496, 43–49, doi:10.1038/nature12003, 2013.

Foster, G. L. et al. Future climate forcing potentially without precedent in the last 420 million years. Nat. Commun. 8, 14845 doi: 10.1038/ncomms14845, 2017.

Furtado, J. C., Di Lorenzo, E., Schneider, N. and Bond, N.A., North Pacific Decadal Variability and Climate Change in the IPCC AR4 Models, American Meteorological Society, Vol. 24, 3049-3067, 2011.

Gulick, S. P. S., Jaeger, J. M., Mix, A. C., Asahi, H., Bahlburg, H., Belanger, C. L.,Berbel., G. B. .B, Childress, L., Cowan, E., Drab, L., Forwick, M., Fukumura, A, Ge, S., Gupta, S., Kiola, A., Konno, S., LeVay, L. J., Marz, C., Matsuzaki, K. M., McClymont, E. L., Moy, C., Müller, J., Nakamura, A., Ojima, T., Ribeiro, F. R., Ridgway, K. D., Romero, O. E., Slagle, A. L., Stoner, J. S., St-Onge, G., Suto, I., Walczak, M. D., Worthington, L. L., Bailey, I., Enkelmann, E., Reece, R. and Swartz, J.M., Mid-Pleistocene climate transition drives net mass loss from rapidly uplifting St. Elias Mountains, Alaska. Proceedings of the National Academy of Sciences of the United States of America, 112(49), 15042–15047. http://doi.org/10.1073/pnas.1512549112, 2015.

Haines, J., and Mazzullo, J., The original shape of quartz silt grains: a test of the validity of the use of quartz grain shape analysis to determine the source of terrigneous silt in marine sedimentary deposits, Marine Geology 78, 227-240, 1988.

Hansen, J., Sato, M., Ruedy, R., Lo, K., Lea, D. & Medina-Elizalde, M., Global temperature change. Proc. Natl Acad. Sci. USA 103, 14 288–14 293, doi:10.1073/pnas.0606291103, 2006.

Harada, N., Sato, M., Shiraishi, A. and Honda, M.C., *Characteristics of alkenone distributions in suspended and sinking particles in the northwestern North Pacific*, Geochim. Cosmochim. Acta, 70, pp. 2045–2062, 2006.

Haug, G. H., Ganopolski, A., Sigman, D. M., Rosell-Mele, A., Swann, G. E. A., Tiedemann, R., Jaccard, S. L., Bollmann, J., Maslin, M A., Leng, M. J. and Eglinton, G., North Pacific seasonality and the glaciation of North America 2.7 million years ago, Nature, vol 433, 821-825, 2005.

Haug, G. H., Sigman, D. M., Tiedemann,R., Pedersen, T. F. and Sarnthein, M., Onset of Permanent stratification in the subarctic Pacific Ocean, Letters to Nature, Vol. 401, 779-782, 1999.

Formatted: Font: 10.5 pt

Formatted: Line spacing: 1.5 lines

Haywood, A.M., Dolan, A.M., Pickering, S.J., Dowsett, H.J., McClymont, E.L., Prescott, C.L., Salzmann, U., Hill, D.J., Hunter, S.J., Lunt, D.J., Pope, J.O., Valdes, P.J., On the identification of a Pliocene time slice for data–model comparison. Philos. Trans. R. Soc., Math. Phys. Eng. Sci. 371, 20120515. http://dx.doi.org/10.1098/ rsta.2012.0515, 2013a.

Haywood, A. M. and Valdes, P. J., Modelling Pliocene warmth: contribution of atmosphere, oceans and cryosphere, Earth and Planetary Science Letters, 218, pp.363-377. doi: 10.1016/S0012-821X(03)00685-X , 2004.

Herbert, Timothy D; Lawrence, Kira T; Tzanova, Alexandrina; Peterson, Laura C; Caballero-Gill, Rocio P; Kelly, Christopher S (Table S2) SST estimates as a function of age, ODP Site 167-1010, PANGAEA, 2018, https://doi.org/10.1594/PANGAEA.885599, In supplement to: Herbert, TD et al., Late Miocene global cooling and the rise of modern ecosystems. Nature Geoscience, 9(11), 843-847, https://doi.org/10.1038/ngeo2813, 2016.

Herbert, Timothy D; Lawrence, Kira T; Tzanova, Alexandrina; Peterson, Laura C; Caballero-Gill, Rocio P; Kelly, Christopher S, (Table S2) SST estimates as a function of age, ODP Site 167-1021. PANGAEA, 2018, https://doi.org/10.1594/PANGAEA.885579, 2018. In supplement to: Herbert, TD et al. Late Miocene global cooling and the rise of modern ecosystems. Nature Geoscience, 9(11), 843-847, https://doi.org/10.1038/ngeo2813, 2016.

Herbert, Timothy D; Lawrence, Kira T; Tzanova, Alexandrina; Peterson, Laura C; Caballero-Gill, Rocio P; Kelly, Christopher S, (Table S2) SST estimates as a function of age, ODP Hole 198-1208A. PANGAEA, 2018, https://doi.org/10.1594/PANGAEA.885584, 2018. In supplement to: Herbert, TD et al., Late Miocene global cooling and the rise of modern ecosystems. Nature Geoscience, 9(11), 843-847, https://doi.org/10.1038/ngeo2813, 2016.

Herbert, Timothy D; Peterson, Laura C; Lawrence, Kira T; Liu, Zhonghui, Plio-Pleistocene tropical alkenone SST reconstructions for ODP Site 138-846. PANGAEA, 2017, https://doi.org/10.1594/PANGAEA.874750, In supplement to: Herbert, TD et al., Tropical Ocean Temperatures Over the Past 3.5 Million Years. Science, 328(5985), 1530-1534, https://doi.org/10.1126/science.1185435, 2010.

Hidy, A. J., Gosse, J. C., Froese, D. G., Bond, J. D., and Rood, D. H.: A latest Pliocene age for the earliest and most extensive Cordilleran Ice Sheet in northwestern Canada, Quaternary Res., 61, 77–84, doi:10.1016/j.quascirev.2012.11.009, 2013.

Hogan, C., *Oceans and Seas Gulf of Alask*a, The Encyclopedia of Earth, http://www.eoearth.org/view/article/153188 (date accessed 13/11/2015), 2013.

Horikawa, K., Martin, E. E., Basak, C., Onodera, J., Seki, O., Sakamoto, T., Ikehara, M., Sakai, S. and Kwamura, K., Pliocene cooling enhanced by flow of low-salinity Bering Sea water to the Arctic Ocean, Nature Communications, 6:7587, 2015.

Jaeger, J.M., Gulick, S.P.S., LeVay, L.J., Asahi, H., Bahlburg, H., Belanger, C.L., Berbel, G.B.B., Childress, L.B., Cowan, E.A., Drab, L., Forwick, M., Fukumura, A., Ge, S., Gupta, S.M., Kioka, A., Konno, S., Marz, C.E., Matsuzaki, K.M., McClymont, E.L., Mix, A.C., Moy, C.M., Müller, J., Nakamura, A., Ojima, T., Ridgway, K.D., Rodrigues Ribeiro, F., Romero, O.E., Slagle, A.L.,Stoner, J.S., St-Onge, G., Suto, I., Walczak, M.H., and Worthington, L.L., 2014. Site U1417. In Jaeger, J.M., Gulick, S.P.S., LeVay, L.J., and the Expedition 341 Scientists, Proc. IODP, 341: College Station, TX (Integrated Ocean Drilling Program). doi:10.2204/iodp.proc.341.103, 2014.

Formatted: Justified, Line spacing: 1.5 lines

Formatted: Font: 10 pt

Deleted: Haug, G. H., Ganopolski, A., Sigman, D. M., Rosell-Mele, A., Swann, G. E. A., Tiedemann, R., Jaccard, S. L., Bollmann, J., Maslin, M A., Leng, M. J. and Eglinton, G., North Pacific seasonality and the glaciation of North America 2.7 million¶
years ago, Nature, vol 433, 821-825, 2005.¶
Haug, G. H., Sigman, D. M., Tiedemann,R., Pedersen, T. F. and Sarnthein, M., Onset of Permanent stratification in the subarctic Pacific Ocean, Letters to Nature, Vol. 401, 779-782, 1999.¶
Haywood, A.M., Dolan, A.M., Pickering, S.J., Dowsett, H.J., McClymont, E.L., Prescott, C.L., Salzmann, U., Hill, D.J., Hunter, S.J., Lunt, D.J., Pope, J.O., Valdes, P.J., On the identification of a Pliocene time slice for data–model comparison. Philos. Trans. R. Soc., Math. Phys. Eng. Sci. 371, 20120515. http://dx.doi.org/10.1098/ rsta.2012.0515, 2013a.¶
Haywood, A. M. and Valdes, P. J., Modelling Pliocene warmth: contribution of atmosphere, oceans and cryosphere, Earth and Planetary Science Letters, 218, pp.363-377. doi: 10.1016/S0012-821X(03)00685-X , 2004.¶

Jansen, E., J. Overpeck, K.R. Briffa, J.-C. Duplessy, F. Joos, V. Masson-Delmotte, D. Olago, B. Otto-Bliesner, W.R. Peltier, S. Rahmstorf, R. Ramesh, D. Raynaud, D. Rind O. Solomina, R. Villalba, and D. Zhang, Palaeoclimate. In Climate Change 2007: The Physical Science Basis. Contribution of Working Group I to the Fourth Assessment Report of the Intergovernmental Panel on Climate Change. S. Solomon, D. Qin, M. Manning, Z. Chen, M. Marquis, K.B. Averyt, M. Tignor, and H.L. Miller, Eds. Cambridge University Press, 433-497, 2007.

Kato, Y., Onodera, J., Suto, I., Teraishi, A. and Takahashi, K., *Pliocene and Pleistocene paleoceanography in the western subarctic Pacific based on diatom analyses of ODP Leg 145 Hole 884B and IODP Expedition 323 Holes U1341B and U1343E*, Deep-Sea Res. II, vol. 125-126, 29-37, 2016.

Knies, J. et al. The emergence of modern sea ice cover in the Arctic Ocean. Nat. Commun. 5:5608 doi: 10.1038/ncomms6608, 2014.

Kornilova, O. and Rosell-Mele, A., Application of microwave-assisted extraction to the analysis of biomarker climate proxies in marine sediments, Organic Geochemistry, 34, 1517–1523, 2003.

Krissek, L. A., Late Cenozoic Ice-Rafting Records From Leg 145 Sites In The North Pacific: Late Miocene Onset, Late Pliocene Intensification and Pliocene-Pleistocene Events, in Rea D. K. Basov, L. A., Scholl, D. W. and Allan, J.F., Proceedings of the Ocean Drilling Scientific Results, Vol 145, 1995.

Lawrence, K. T., Herbert, T. D., Brown, C. M., Raymo, M. E. and Haywood, A. M., High-amplitude variations in North Atlantic sea surface temperature during the early Pliocene warm period, Paleoceanography, 24, PA2218, https://doi.org/10.1029/2008PA001669, 2009.

Lawrence, K. T., Sosdian, S., Wite, H. E. and Rosenthal, Y., North Atlantic climate evolution trough the Plio-Pleistocene climate transitions, Earth and Planetary Science Letters 300, 329-342, 2010.

Lisiecki, Lorraine E; Raymo, Maureen E, Pliocene-Pleistocene stack of globally distributed benthic stable oxygen isotope records. PANGAEA, https://doi.org/10.1594/PANGAEA.704257,2005. Supplement to: Lisiecki, LE; Raymo, ME, A Pliocene-Pleistocene stack of 57 globally distributed benthic d18O records. Paleoceanography, 20, PA1003, https://doi.org/10.1029/2004PA001071, 2005.

Livsey, D.N., Simms, A.R., Clary, W.G., Wellner, J.S., Anderson, J.B., and Chandler, J.P., Fourier grain-shape analysis of Antarctic marine core: the relative influence of provenance and glacial activity on grain shape, Journal of Sedimentary Research 83, 80-90, 2013.

Locarnini, R. A., A. V. Mishonov, J. I. Antonov, T. P. Boyer, H. E. Garcia, O. K. Baranova, M. M. Zweng, C. R. Paver, J. R. Reagan, D. R. Johnson, M. Hamilton, and D. Seidov, 2013. *World Ocean Atlas 2013, Volume 1: Temperature.* S. Levitus, Ed., A. Mishonov Technical Ed.; NOAA Atlas NESDIS 73, 40 pp.

Martínez-Botí, M. A., Foster, G. L. Chalk, T. B., Rohling, E. J., Sexton, P. F., Lunt, D. J., Pancost, R. D., Badger, M. P. S., Schmidt. D. N., Plio-Pleistocene climate sensitivity evaluated using high-resolution CO2records. Nature, 518 (7537): 49 DOI: 10.1038/nature14145, 2015.

Martínez-García, A., Rosell-Mele, A., McClymont, E.L., Gersonde, R. & Haug, G. Subpolar Link to the Emergence of the Modern Equatorial Pacific Cold Tongue, Science, 328: 1550-1553, 2010.

Martínez-García, Alfredo; Rosell-Melé, Antoni; McClymont, Erin L; Gersonde, Rainer; Haug, Gerald H, (Table S3) Sea surface temperature and relative abundance of $C_{37:4}$ alkenone in ODP Site 145-882. PANGAEA, https://doi.org/10.1594/PANGAEA.771707, 2010. In supplement to: Martínez-García, A et al. (2010): Subpolar Link to the Emergence of the Modern Equatorial Pacific Cold Tongue. Science, 328(5985), 1550-1553, https://doi.org/10.1126/Science.1184480.

Martrat, B., Grimalt, J. O., Shackleton, N. J., de Abreu, L., Hutterli, M. A. and Stocker, T. F., *Four Climate Cycles of Recurring Deep and Surface Water Destabilizations on the Iberian Margin*, Science Volume 317, 5837, 502-507, 2007.

März, C., Schnetger, B., and Brumsack, H.-J2013, Nutrient leakage from the North Pacific to the Bering Sea (IODP Site U1341) following the onset of Northern Hemispheric Glaciation?, Paleoceanography, 28, 68–78, doi:10.1002/palo.20011, 2013.

Deleted: ¶

Maslin, M.A., Haug, G.H., Sarnthein, M., Tiedemann, R., The progressive in- tensification of Northern Hemisphere glaciation as seen from the North Pacific, Geol. Rundsch 85, 452–465, 1996.

Matthews, J., The Assessment of a Method for the Determination of Absolute Pollen Frequencies. New Phytologist 68, 161–166, 1969, https://doi.org/10.1111/j.1469-8137.1969.tb06429.x.

Matthiessen, J., Knies, J., Vogt, C. and Stein, R., Pliocene palaeoceanography of the Arctic Ocean and subarctic seas, Phil. Trans. R. Soc. A (2009) 367, 21–48 doi:10.1098/rsta.2008.0203, 2008.

McCalpin, J. P., Bruhn, R. L., Pvlis, T. L., Gutierres, F., Guerrero, J. and Lucha, P., Antislope scarps, gravitational spreading, and tectonic faulting in the western Yakutat microplate, south coastal Alaska, Geosphere, 7 (5): 1143-1158, 2011.

McClymont, E.L., Elmore, A.C., Kender, S., Leng, M.J., Greaves, M. and Elderfield, H., Pliocene-Pleistocene evolution of sea surface and intermediate water temperatures from the southwest Pacific, Paleoceanography, 31, 895-913, 2016.

McClymont, E.L., Rosell-Melé, A., Haug, G. and Lloyd, J.M., *Expansion of subarctic water masses in the North Atlantic and Pacific oceans and implications for mid-Pleistocene ice sheet growth*, Paleoceanography, 23, PA4214, 2008.

Meheust, M., Fahl, K. and Stein, R., Variability in modern sea surface temperature, sea ice and terrigenous input in the sub-polar North Pacific and Bering Sea: Reconstruction from biomarker data, Organic Geochemistry 57, 54-64, 2013.

Mertens, K.N., Verhoeven, K., Verleye, T., Louwye, S., Amorim, A., Ribeiro, S., Deaf, A.S., Harding, I.C., De Schepper, S., González, C., Kodrans-Nsiah, M., De Vernal, A., Henry, M., Radi, T., Dybkjaer, K., Poulsen, N.E., Feist-Burkhardt, S., Chitolie, J., Heilmann-Clausen, C., Londeix, L., Turon, J.L., Marret, F., Matthiessen, J., McCarthy, F.M.G., Prasad, V., Pospelova, V., Kyffin Hughes, J.E., Riding, J.B., Rochon, A., Sangiorgi, F., Welters, N., Sinclair, N., Thun, C., Soliman, A., Van Nieuwenhove, N., Vink, A., Young, M., Determining the absolute abundance of dinoflagellate cysts in recent marine sediments: The Lycopodium marker-grain method put to the test. Review of Palaeobotany and Palynology 157, 238–252, 2009, https://doi.org/10.1016/j.revpalbo.2009.05.004.

Molnia, B.F., *Glaciers of North America -- Glaciers of Alaska*, in Williams, R.S., Jr., and Ferrigno, J.G., eds., Satellite image atlas of glaciers of the world: U.S. Geological Survey Professional Paper 1386-K, 525 p, 2008.

Mudelsee, M. and Raymo, M. E., Slow dynamics of the Northern Hemisphere glaciation, Paleoceanography, vol 20, PA4022, 2005.

Müller P. J., Kirst G., Ruhland G., von Storch I., and RosellMelé A., Calibration of the alkenone paleotemperature index UK37' based on core-tops from the eastern South Atlantic and the global ocean (608 N–608 S), Geochim. Cosmochim. Acta 62, 1757–1772, doi:10.1016/S0016-7037(98)00097-0, 1998.

Müller, J., Romero, O. Cowan, E. A., McClymont, E. L., Forwick, M., Asahi, H., Marz, C., Moy, C. M., Suto, I., Mix, A. and Stoner, J., Cordilleran ice-sheet growth fueled primary productivity in the Gulf of Alaska, northeast Pacific Ocean, Geology, v. 46; no. 4; p. 307–310, 2018.

Naafs, B. D. A., Hefter, J., Acton, G., Haug, G. H., Martínez-García, A., Pancost, R. and Stein, R., Strengthening of the North American dust sourcesduring the late Pliocene (2.7 Ma), Earth and Planetary Science Letters 317-318, 8-19, http://dx.doi.org/10.1016/j.epsl.2011.11.026, 2012.

Nie, J. et al. Pacific freshening drives Pliocene cooling and Asian monsoon intensification. Sci. Rep. 4, 5474; DOI:10.1038/srep05474, 2014.

Pagani, M., Liu, Z., La Riviere, J. and Ravelo, A. C., High Earth-system climate sensitivity determined from Pliocene carbon dioxide concentrations, Nature Geoscience, Vol 3., 27-30, 2010.

Pickart, RS, Macdonald, A. M., Moore, G. W. K., Renfrew, I. A., Walsh, J. E. and Kessler, W. S., 2009, *Seasonal evolution of Aleutian low pressure systems: implications for the North Pacific subpolar circulation*. J Phys Oceanogr 39, 1317– 1339, 2009.

Powell, R. D., and Molnia, B. F., Glacimarine sedimentary processes, facies and morphology of the south-southeast Alaska shelf and fjords, Mar. Geol., 85, 359–390, doi:10.1016/0025-3227(89)90160-6, 1989.

Prahl F. G., Muehlhausen L. A., and Zahnle D. L., Further evaluation of long-chain alkenones as indicators of paleoceanographic conditions, Geochim. Cosmochim. Acta 52, 2303–2310, 1988.

Prueher, Libby M; Rea, David K: (Table 1) Age, magnetic susceptibility, and mass accumulation rate of volcanic glass and IRD from ODP Site 145-887. PANGAEA, https://doi.org/10.1594/PANGAEA.706309, 2001.

Raymo, M. E., Grant, B., Horowitz, M. and Rau, G. H., Mid-Pliocene warmth: stronger greenhouse and stronger conveyor, Marine Micropalaeontology 27, 313-326, 1996.

Rea, D. K., Basov, I. A., Krissek, L. A. and the Leg 145 Scientific Party, *Scientific Results of drilling the North Pacific Transect*, in Rea, D. K., Basov, I. A., Scholl, D. W and Allan, J. F., 1995, Proceedings of the Ocean Drilling Program, Scientific Results, VOL 145, 1995.

Rea, D. K., Snoeckx, H. & Joseph, L. H. Late Cenozoic eolian deposition in the North Pacific: Asian drying, Tibetan uplift, and cooling of the northern hemisphere. *Paleoceanography* 13, 215–224, 1998.

Reece, R. S., Gulick, S. P. S., Horton, B. K., Christeson, G. L. and Worthington, L. L., Tectonic and climatic influence of the evolution of the Surveyor Fan and Channel system, Gulf of Alaska, Geosphere 7, 830-844, 2011.

Rosell-Melé, A., Carter, J. F., Parry, A. T. and Eglinton, G., *Determination of the UK37 Index in Geological Samples*, Analytical Chemistry, 67, 1283-1289, 1995.

Rodionov, S. N., Bond, N. A. and Overland, J. E., The Aleutian Low, storm tracks, and winter climate variability in the Bering Sea, Deep Sea Res., Part II, 54, 2560–2577, doi:10.1016/j.dsr2.2007.08.002, 2007.

Salzmann, U., Williams, M., Haywood, A. M. Johnson, A. I. A, Kender, S. and Zalasiewicz, J., Climate and environment of a Pliocene warm world, Palaeogeography, Palaeoclimatology, Palaeoecology, 309, 1-8, 2011.

Sánchez-Montes, M. L.; McClymont, E. L; Lloyd, J. M; Müller, J.; Cowan, E. A; Zorzi, C., Alkenone sea surface temperatures, ice rafted debris, terrestrial/aquatic n-alkane ratio, pollen counts and a new age and depth models from IODP Expedition 341 Site U1417, Gulf of Alaska. PANGAEA, 2019, https://doi.org/10.1594/PANGAEA.899064 (dataset in review).

Sarnthein, M., Schneider, B. and Grootes, P. M., Peak glacial ^{14}C ventilation ages suggest major draw-down of carbon into the abyssal ocean. Climate of the Past, 9, 2595-2614, 2013.

Schlitzer, R., Ocean Data View, odv.awi.de, 2018.

Seki, O., Foster, G. J., Schmidt, D. N., Mackensen, A., Kawamura, K. and Pancost, R. D., Alkenone and boron-based Pliocene pCO2 records, Earth and Planetary Science Letters 292, 201-211, doi:10.1016/j.epsl.2010.01.037, 2010.

Seki, Osamu; Foster, Gavin L; Schmidt, Daniela N; Mackensen, Andreas; Kawamura, Kimitaka; Pancost, Richard D, Alkenone and boron based Oligocene pCO2 records. PANGAEA, https://doi.org/10.1594/PANGAEA.732923, 2010. Supplement to: Seki, O., Foster, G. J., Schmidt, D. N., Mackensen, A., Kawamura, K. and Pancost, R. D.,Alkenone and boron based Pliocene pCO2 records. Earth and Planetary Science Letters, 292 (1-2), 201-211, https://doi.org/10.1016/j.epsl.2010.01.037, 2010.

Spies, R. B., *Long-term Ecological Change in the Northern Gulf of Alaska*, Elsevier, ISBN 978-0-444-52960-2, 2007.

St. John, K.E.K and Krissek, L.A., Regional patterns of Pleistocene ice-rafted debris flux in the North Pacific. Paleoceanography, Vol. 14, 653-662, 1999.

Swann, G. E. A., Snelling, A. M. and Pike, J., Biogeochemical cycling in the Bering Sea over the onset of major Northern Hemisphere Glaciation, Paleoceanography, 31, doi:10.1002/ 2016PA002978, 2016.

Tierney, J. E., and Tingley, M. P., BAYSPLINE: A new calibration for the alkenone paleothermometer. Paleoceanography and Paleoclimatology, 33, 281–301, 2018.

Zachos, J., M. Pagani, L. Sloan, E. Thomas, and K. Billups, Trends, rhythms, and aberrations in global climate 65 Ma to present,Science, 292(5517), 686–693, 2001a.

Walinsky, S.E., Prahl, F.G., Mix, A.C., Finney, B.P., Jaeger, J.M., and Rosen, G.P., *Distribution and composition of organic matter in surface sediments of coastal southeast Alaska*. Cont. Shelf Res., 29, 13, 1565–1579, doi:10.1016/j.csr.2009.04.006, 2009.

Weingartner, T., *Chapter 2.2: The physical environment of the Gulf of Alaska*. In: Spies, R.B. (Ed.), Long-term Ecological Change in the Northern Gulf of Alaska. Elsevier, Oxford, p. 589, 2007.

Weingartner, T, Danienlson, S., Shipton, P and Leech, D, *GAK 1 Time Series*, access online http://www.ims.uaf.edu/gak1/, last date accessed 23/12/2016, 2016.

Willeit, M., Ganopolski, A., Calov, R., Robinson, A. and Maslin, M., The role of CO2 decline for the onset of Northern Hemisphere glaciation, Quaternary Science Reviews 119 (2015) 22e34, 2015.

Table 1: Average SST (°C) and %$C_{37:4}$ during key climatic intervals 4.0-3.0 Ma, 3.0-2.8 Ma, 2.7-2.4 Ma, 2.4-1.7 Ma. Average SST (°C) is the average of all the data points of the time interval, peak SST (°C) average is the average of the highest data points of each interval selected (Fig. 2), trough SST (°C) average is the average of the lowest data points of each interval (Fig. 5.2) and the average SST (°C) variability is the difference between average SST peak and the average SST trough. In black: data calculated from U^{K}_{37} (Prahl *et al*., 1988) and in black bold, data from U^{K}_{37}' (Müller *et al*., 1998).

Age intervals (Ma)	Average SST (°C)	Peak SST (°C) average	Trough SST (°C) average	Average SST variability (°C)	Average $C_{37:4}$ (%)	Peak $C_{37:4}$ (%)
4.0-3.1	10.2/**8.7**	12.5/**11.4**	7.2/**4.4**	5.3/**7.0**	1.9	10.5
3.1-2.8	8.5/**7.3**	9.9/**9.0**	7.4/**5.7**	2.4/**3.3**	3.9	4.9
2.7-2.4	10.2/**9.8**	13.2**12.6**	8.4/**6.6**	4.8/**5.9**	4.8	24.1
2.4-1.7	9.0/**8.6**	10.7/**10.4**	6.8/**4.8**	3.9/**5.6**	5.2	23.8
4-2.8 Ma	9.6/**8.2**	11.2/**10.2**	7.3/**5.1**	3.9/**5.2**	2.5	10.5
2.7-1.7Ma	9.6/**9.1**	12.0/**11.5**	7.6/**5.7**	4.4/**5.8**	5.0	24.1

Formatted: Space Before: 0 pt, Line spacing: 1.5 lines

Deleted: ¶

Deleted: **Table 2: Extent of SST range and influence across core sites of Fig. 3.** SST cooling or warming at significant climate intervals: the cooling Pliocene prior the M2 event, the MG1-Gi1 warming, the M2 cooling event, the onset of the NHG, the intensification of the NHG and the period after the NHG during the early Pleistocene. Cells highlighted in red and blue shading are highest SST range (darker red or blue) to lesser degree of SST range (lighter red or blue) of each interval.¶
Time intervals ... [6]

Supplement information

A shipboard composite depth scale was generated for Site U1417 to take into account the recovery of sediments from multiple holes. A continuous "splice" spanning the upper and middle Pleistocene sediments was generated from 0-224.2 m core composite depth ("CCSF-A"; Jaeger *et al.,* 2014). Below this depth, and especially where coring switched from the APC (advanced piston corer) to the XCB (extended core barrel) system, core recovery was reduced from ~97 % (APC) to ~37 % (XCB). The recovered sediments tended to be in "biscuits" of coherent sediment; without knowledge of where these biscuits had originally been distributed within the 9.5 m core, they were grouped into the uppermost portions of each core (e.g. if 3 m of sediments were recovered, they were placed into the 0-3 m depth interval for each core). This leads to a clustering of recovered sediment and proxy data (Fig. S1 and Fig. S2). There is a possibility that recovery problems such as movement of sediment through the liner during sediment recovery and logging resulted in difficulties for sediment depth attribution during IODP Expedition 341. Jaeger *et al*., (2014) acknowledge that "*In areas of lower core recovery, the exact lithostratigraphic unit boundaries may have an error range of a few meters due to recovered intervals being assumed to reside at the top of each cored interval […]*" [Jaeger *et al*., (2014); Core Log Seismic integration section].

This problem was also been observed, and accounted for, during ODP Leg 181 at Site 1123 (Shipboard Scientific Party, 2000). In this instance, correlations were made between magnetic susceptibility measured in the recovered XCB cores and measured by the logging of the drilled hole. The results confirmed that the recovered "biscuits" were likely to have been distributed through each of the recovered core depths, rather than clustering in the upper few metres (Shipboard Scientific Party, 2000). However, Jaeger *et al*., (2014) had already considered this method during the development of the preliminary age model: "*We combined sediment core observations and physical properties data with downhole logging data from Site U1417 to (1) evaluate how representative the recovered cores are relative to the portion of the sedimentary section that was logged, (2) determine the nature and extent of sediment not recovered in the XCB/RCB drilling process, and (3) examine whether observed sedimentary units and features can be correlated to borehole data and ultimately be described at higher vertical resolution at Site U1417*" [Jaeger *et al*., (2014); Core Log Seismic integration section; Lithostratigraphy–downhole logging data integration subsection]. Having compared magnetic susceptibility measurements from both recovered cores and logging operations, correlation problems were noted, linked to the presence of diamicts and poor recoveries (as low as 21 %) for some cores (Jaeger *et al*., 2014).

Deleted: the

Deleted: the

To test the impact of the assumption that sediment recovered belonged to the top core (the 'shipboard age model'), we propose a new CCSF-A depth model in response to evenly distributing sediment samples across each of the cores examined here, according to the methods outlined by Shipboard Scientific Party (2004) for ODP 1123. Our samples are linearly distributed between fixed sample CCSF-A depths at the top and bottom of each core. We continue to apply the age-depth

Deleted: S

relationships generated by the shipboard age model respecting the magnetostratigraphic chronozones in Jaeger *et al.* (2014) to convert depth to age. The Gauss/Matuyama boundary at 2.581 Ma was clearly identified in Holes U1417B, U1417D and U1417E. Less confidence in identifying events below this reflect the impact of poor core recovery and the formation of the core biscuits (Jaeger *et al*., 2014).

New age model:

All samples presented in this study are from Hole U1417D with the exception of a single sample (U1417C 25H-3, shipboard average CCSF-A depth of 250.817 m) (Fig. S1). The constrained magnetostratigraphic chronozone and sub-chronozone events found in Core U1417D are limited to C2r.1n (T) Reunion, C2An.1n (T) Gauss/Matuyama and the transition of C2An.3n (B) Gilbert/Gauss (Jaeger *et al.* 2014). Jaeger *et al.* (2014) propose a unified magnetostratigraphic ages and depths across U1417 cores using the composite depth scale "CCSF-A" (Fig. S1). Cores 26H-36X appear in continuous sedimentation in shipboard photographs and with no major core recovery losses. Therefore, the stretched model at these samples copies the shipboard age/depth model. Core 39X contains important gaps in sediment recovery, but the sediment recovered above our sample appears uninterrupted from the top core in the same "biscuit". This sample is kept on the shipboard age/depth. Our two samples at core 40X were also interpreted as being part of the same biscuit by revising the core photographs. The distance between these samples were respected when applying the stretched age model. The ages/depths of samples contained in 41X-54X are stretched linearly downcore between top core and bottom core ages/depths. These top and bottom core ages and depths are fixed as tie points (Fig. S3B). The two last samples at core 54X keep the shipboard age/depth model for not having sampled sediment for biomarker analyses below U1417D 55X to follow our interpolation with the same criteria. The new stretched ages for the magnetic reversals at Site U1417 remain closest to the chronozone interpretations of Jaeger *et al*., (2014) when comparing with the Geological Time Scale 2012 (Gradstein *et al.*, 2012) magnetic reversals (Fig. S2 and S3a). The Olduvai and Reunion magnetic reversals are maintained as with the shipboard age model. The new Gauss/Matuyama magnetic reversal stretched age is similar than the shipboard age model, however, the Gilbert/Gauss transition moves from 3.75 Ma following shipboard age model to 3.88 Ma in our new stretched age model (Fig. S2b and d and S3a). The Gilbert/Gauss transition was only found in Hole U1417D and due to its depth and poor core recovery it does not represent a robust tie point to control our new age model. Our new age and depth models add detail in the sedimentation rates at Site U1417 (Fig. S3b). The comparison of our stretched age model with the LR04 benthic stack (Lisiecki and Raymo, 2005) suggests that the new age model preserves, or even enhances, the expression of glacial-interglacial climate variability which was not immediately visible from the original depth model (Fig. S2).

Deleted: and

Deleted: age and depth

Deleted: the same as

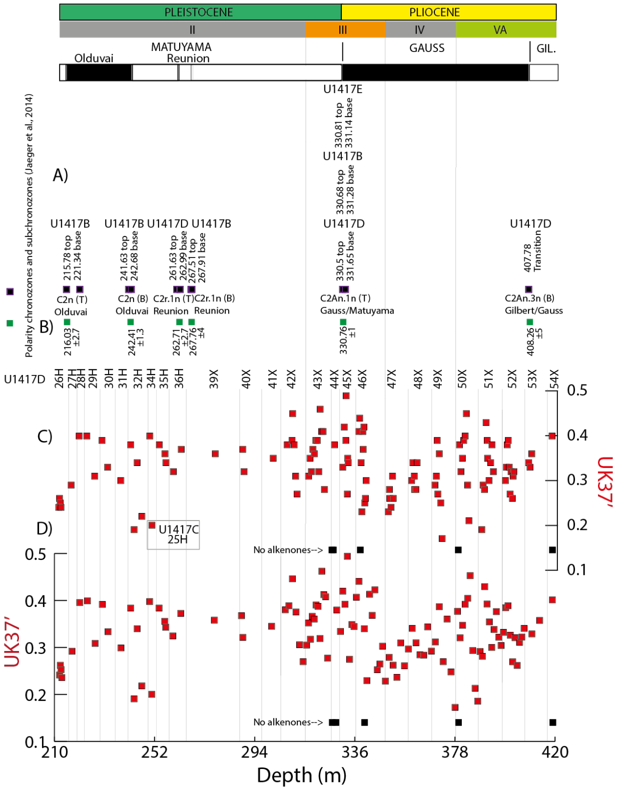

Figure S1: Comparison between shipboard depth model (Jaeger *et al.*, 2014) and the depth model presented in this paper. On top, Pliocene and Pleistocene division by the Gauss/Matuyama magnetic reversal, lithostratigraphic units and colours as detailed in the main text and Site U1417 choronozone interpretations of (Jaeger *et al.,* 2014), a) magnetostratigraphic chronozone and subchronozones depths and interpretations present in different holes (Jaeger *et al.,* 2014), b) Site U1417 unified magnetostratigraphic chronozone interpretations (Jaeger *et al.,* 2014), d) U$^{K}_{37}$' at Site U1417 plotted against the preliminary CCSF-A depths of (Jaeger *et al.,* 2014) and e) U$^{K}_{37}$' at Site U1417 plotted against the new stretched depths. Black squares=samples with no alkenones. Shorter grey vertical lines indicate separation between U1417D cores and longer grey vertical lines indicate lithology unit boundaries. Grey square delimits the only sample belonging to Hole U1417C.

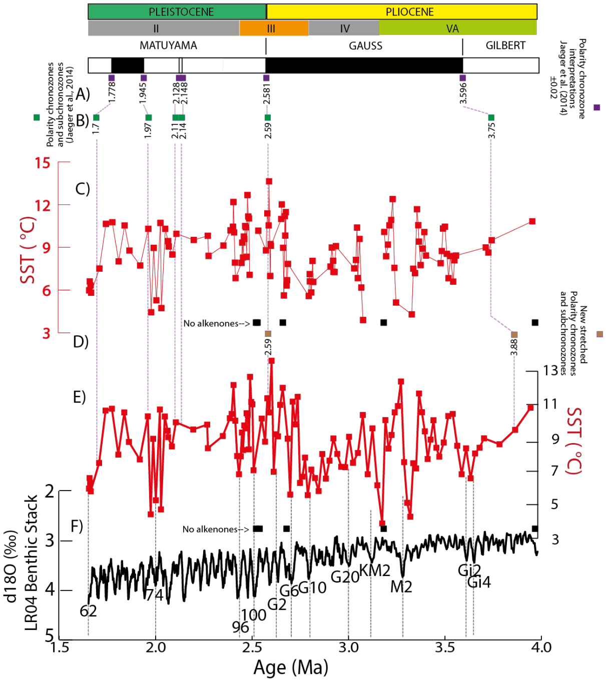

Figure S2: Sea surface temperatures of U1417 plotted with the new age model proposed here and compared to the LR04 (Lisiecki and Raymo, 2005). On top, Pliocene and Pleistocene division, lithostratigraphic units and colours as detailed in the main text and the magnetostratigraphic chronozone interpretation (Jaeger *et al.,* 2014) a) polarity chronozone interpretation ages (Jaeger *et al.,* 2014), b) polarity chronozone interpretation ages calculated from the CCSF-A of Figure S1, c) SST (calculated from Müller *et al.,* 1998 calibration) at Site U1417 plotted against the shipboard age model of (Jaeger *et al.,* 2014), d) polarity chronozone interpretation ages according to our new stretched model, e) SST (calculated from Müller *et al*., 1998 calibration) at Site U1417 plotted against the new stretched age model and f) LR04 benthic stack (Lisiecki and Raymo, 2005) and distinctive marine isotope stadials. Black squares represent samples with no alkenones and purple vertical lines represent the correlation of magnetostratigraphic chronozone ages across panels.

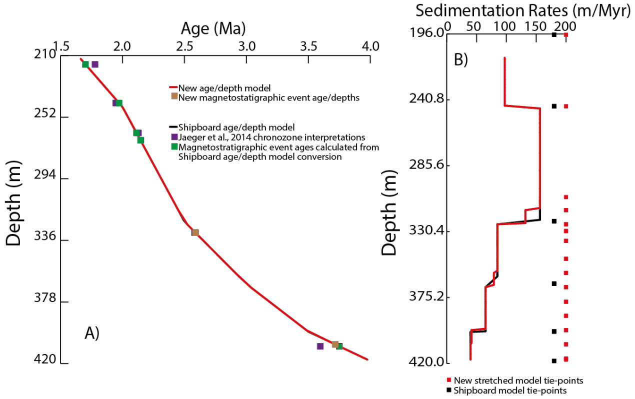

Figure S3: Shipboard and new age/depth model comparisons. a) shipboard (black line, Jaeger *et al.,* 2014) and new stretched (red line) age/depth models. Magnetostratigraphy chronozone interpretations depth and ages as assigned in Jaeger *et al.,* 2014 (purple squares), Magnetostratigraphy chronozone calculated ages from the shipboard CCSF-A depth/age model of Jaeger *et al*., 2014 and ages calculated according to the new stretched age model (brown squares); b) average sedimentation rates (m Myr^{-1}) with the detailed tie points considered following the shipboard (in black) and new stretched (in red) age/depth models.

References

Gradstein, F.M., Ogg, J.G., Schmitz, M., Ogg, G., *The geologic time scale 2012*, Elsevier, 2012.

Jaeger, J.M., Gulick, S.P.S., LeVay, L.J., Asahi, H., Bahlburg, H., Belanger, C.L., Berbel, G.B.B., Childress, L.B., Cowan, E.A., Drab, L., Forwick, M., Fukumura, A., Ge, S., Gupta, S.M., Kioka, A., Konno, S., Marz, C.E., Matsuzaki, K.M., McClymont, E.L., Mix, A.C., Moy, C.M., Müller, J., Nakamura, A., Ojima, T., Ridgway, K.D., Rodrigues Ribeiro, F., Romero, O.E., Slagle, A.L., Stoner, J.S., St-Onge, G., Suto, I., Walczak, M.H., and Worthington, L.L., *Site U1417*, 2014. In Jaeger, J.M., Gulick, S.P.S., LeVay, L.J., and the Expedition 341 Scientists, Proc. IODP, 341: College Station, TX (Integrated Ocean Drilling Program). doi:10.2204/iodp.proc.341.103, 2014.

Lisiecki, Lorraine E; Raymo, Maureen E, Pliocene-Pleistocene stack of globally distributed benthic stable oxygen isotope records. PANGAEA, https://doi.org/10.1594/PANGAEA.704257,2005. Supplement to: Lisiecki, LE; Raymo, ME, A Pliocene-Pleistocene stack of 57 globally distributed benthic d18O records. Paleoceanography, 20, PA1003, https://doi.org/10.1029/2004PA001071, 2005.

Müller P. J., Kirst G., Ruhland G., von Storch I., and Rosell-Melé A., Calibration of the alkenone paleotemperature index U^{K}_{37}' based on core-tops from the eastern South Atlantic and the global ocean (608 N–608 S), Geochim. Cosmochim. Acta 62, 1757–1772, doi:10.1016/S0016-7037(98)00097-0, 1998.

Shipboard Scientific Party, Site 1123: North Chatham Drift – a 20 Ma Record of the Pacific Deep Western Boundary Current, 2000. In Carter, R.M., McCave, I.N., Richter, C., Carter, L., et al., *Proc. ODP, Init. Repts.,* 181, 1–184.